"Gamma Ray Astronomy"

FINAL REPORT

Contract NAS8-38609
Delivery Order Number 90

July 27, 1993 – March 27, 1994

Prepared by

Dr. William S. Paciesas

Prepared for
George C. Marshall Space Flight Center
National Aeronautics and Space Administration
Marshall Space Flight Center, Alabama 35812

Submitted by
Department of Physics
The University of Alabama in Huntsville
Huntsville, Alabama 35899

March 1994

1. INTRODUCTION

The Burst and Transient Source Experiment (BATSE) is one of four instruments on the Compton Observatory which was launched by the space shuttle Atlantis on April 5, 1991. As of mid-March, 1994, BATSE detected more than 925 cosmic gamma-ray bursts and more than 725 solar flares. Pulsed gamma-rays have been detected from at least 16 sources and emission from at least 28 sources (including most of the pulsed sources) has been detected by the Earth occultation technique. UAH participation in BATSE is extensive but can be divided into two main areas, operations and data analysis. The daily BATSE operations tasks represent a substantial level of effort and involve a large team composed of MSFC personnel as well as contractors such as UAH. The scientific data reduction and analysis of BATSE data is also a substantial level of effort in which UAH personnel have made significant contributions.

2. MISSION OPERATIONS

W. Paciesas served as BATSE Mission Operations Software (MOPS) Development Manager, chairing the Level V Configuration Control Board for the MOPS software. Paciesas also supervised distribution of the Individual Burst Data Base (IBDB) files to co-investigators at Goddard Space Flight Center (GSFC) and the University of California, San Diego (UCSD), and to the CGRO Science Support Center. K. Squier provided maintenance of software to produce summary reports of Individual Burst Data Base (IBDB) contents for selected triggers. Squier also continued development of software to update certain IBDB contents and/or produce additional IBDB files without regenerating the entire IBDB for a particular trigger. Z. Shariff and G. Richardson assisted in BATSE data operations on a regular basis. Shariff, Richardson, T. Koshut, R. Mallozzi, and J. Brainerd performed burst operations regularly.

Paciesas led an effort to plan replacement of the MOPS burst catalog with an improved trigger catalog. A new structure and organization for the catalog was developed in consultation with various BATSE science team members. Paciesas wrote a Software Change Plan to implement the catalog with a minimum of impact on normal operations. Squier devloped code for initial conversion of the old MOPS catalog into the new format.

V. Chaganti assumed responsibility for maintenance of the HER/SHER correction software. His first task involved correction of the first HERB/SHERB readout records and merging of these into the corrected HER/SHER files.

4. BURST DATA ANALYSIS

Paciesas, Pendleton, Mallozzi and Koshut were part of the collaborative effort to produce the first BATSE catalog of gamma-ray bursts.[1] Pendleton was primarily responsible for calculation of burst fluxes and fluences, while Koshut had primary responsibility for calculation of burst durations. The durations were shown to have a bimodal distribution[2] with a minimum around 1–2 s. To investigate this further, Koshut led a preliminary study contrasting the properties of short events with short spikes in long events.[3]

Pendleton, Koshut and Chaganti developed software to be used for production of the second burst catalog. Improvements to the existing algorithms for calculation of burst fluxes, fluences, and durations were implemented and a user-friendly interface developed. The ultimate goal is produce these numbers routinely as part of daily burst operations rather than as a later production data analysis task. Chaganti and Shariff completed production of fluxes and fluences for the second catalog using this software. Koshut and Mallozzi completed production of most time duration measurments using this software. In a related effort for the second catalog, Koshut led a study of systematic errors in the location of bursts using the MAXBC datatype.[4]

Paciesas coordinated BATSE spectral analysis efforts among UAH, MSFC, GSFC, and UCSD and supervised the time-resolved burst spectroscopy key project. Visual searches for spectral features in BATSE bursts were continued as part of this project. No convincing evidence has yet been found for such features;[5] a candidate line found in one burst is probably spurious.[6,7] The lack of line features cannot yet be considered inconsistent with other observations.[8,9] An automated procedure for exhaustive searches for line features is being implemented.[10] Studies of burst continuum spectra showed differences among bursts as to their temporal evolution.[11-14] The spectroscopy collaboration also produced a catalog of burst spectra.[15]

Pendleton led studies of continuum spectral characteristics of gamma-ray bursts using low-energy-resolution data (4 channels)[16] and medium-energy-resolution (16 channels).[17] Pendleton collaborated with GRO Guest Investigator (GI) E. Fenimore (Los Alamos Nat. Lab.) and others on deriving and interpreting the number/intensity distribution of gamma-ray bursts obtained by combining BATSE and PVO data.[18]

UAH personnel were involved in various studies of burst sky distributions. Brainerd led a collaboration which found no significant clustering of bursts using a nearest-neighbor analysis.[19] Koshut and Mallozzi worked with other BATSE team members to put limits on heliocentric models for bursts.[20] Pendleton and Paciesas collaborated with J. Hakkila (Mankato St. U.) and others on constraining galactic burst models from BATSE data.[21]

Pendleton, Paciesas and Koshut collaborated with C. Kouveliotou (MSFC/USRA) and others in analysis of recurrent events detected by BATSE from the soft gamma repeater SGR 1900+14.[22] Pendleton and Paciesas also collaborated in studies led by Kouveliotou of events from SGR 1806-20[23] and the unusually intense event GRB930131.[24]

Paciesas worked with I. Mitrofanov (Space Research Inst., Moscow), J. Norris (NASA/GSFC) and others on searches for time dilation effects in bursts which would be expected if they are cosmological in origin. The results so far are suggestive but not conclusive.[25,26]

Brainerd developed a model for burst spectra from sources at comological distances based on Compton scattering in a relatively thick obscuring medium[27,28] and studied effects which might mimic cosmological time dilation of bursts in Euclidian space.[29]

5. NON-BURST DATA ANALYSIS

Paciesas and Mallozzi worked on occultation analysis of selected sources. Mallozzi searched for low-energy gamma-ray emission from a set of active galactic nuclei (AGNs) detected by EGRET.[30] Paciesas led analysis of temporal and spectral variability of the quasar 3C 273[31] and the transient source Nova Muscae.[32] Paciesas analyzed the intensity dependence of Cygnus X-1 spectral states around a period of unusually low intensity in

January-February 1994.[33] Paciesas and Pendleton collaborated with various other BATSE team members on studies of the galactic black-hole candidate GX 339-4, the transient sources GRO J1719-24 and GRS 1009-45, and sources in the galactic center region.[34-36] Paciesas collaborated with the effort led by S. N. Zhang (USRA) to develop a method for producing images from occultation data.[37-39] Paciesas collaborated with J. Greiner (MPE Garching) on analysis of the transient GRS 1915+105[40] and with J. Ling (JPL) on analysis of Cygnus X-1.[41]

M. Stollberg continued analysis of data from the x-ray binary EXO 2030+375 as part of his Ph. D. dissertation.[42] Stollberg also assisted the BATSE team in production pulsar analysis and worked on documentation of pulsar timing analysis algorithms. Stollberg and Pendleton collaborated with R. Wilson (MSFC) and others in analysis of the transient pulsar GRO J1008-57.[43,44] Pendleton collaborated with Wilson and others on a study of intensity/torque correlations in Her X-1.[45,46] Paciesas collaborated with B. Rubin (USRA) and others on an investigation of the long-period pulsar 4U 1538-52.[47]

Paciesas and Pendleton continued to work with various other CGRO Guest Investigators in ongoing studies. These included A. Parsons (NASA/GSFC), R. Edelson (Univ. of Iowa) and M. Machado (UAH).

5. OTHER ACTIVITIES

Brainerd and Pendleton served on the local organizing committee for the Gamma-Ray Burst Workshop held in Huntsville on 20–22 October 1993. Brainerd co-edited the workshop proceedings, along with G. FIshman (MSFC) and K. Hurley (UC Berkeley). Paciesas, Pendleton and Mallozzi presented contributed papers at the Second Compton Symposium in College Park, MD, during 20–22 September 1993. Paciesas presented an invited talk on "CGRO/BATSE occultation studies of galactic black hole candidates and AGNs" at the workshop on *Pairs, Gamma-Rays and Black Holes* in Koninki, Poland, during 5–8 October 1993. Stollberg and Paciesas presented contributed papers at the conference on *The Evolution of X-Ray Binaries* in College Park, MD, during 11–13 October 1993. Paciesas presented invited lectures on "BATSE Observations of Extragalactic Objects" and "BATSE Observations of Galactic Compact Objects" at the NATO Advanced Study Institute on *The Gamma-Ray Sky from Compton/GRO and Sigma* in Les Houches, France,

during 25 January-4 February 1994.

Paciesas continued to serve as BATSE representative to the CGRO User's Committee, attending the meeting on 23–24 September 1993. Paciesas reviewed and provided updated BATSE inputs to the CGRO Project Data Management Plan and to the NASA Research Announcement for phase 3 of the GI program.

Meetings of the Burst Spectroscopy Team were held on 9–10 September 1993 at GSFC and on 17-18 February 1994 at UCSD (both were attended by Paciesas and Pendleton).

Copies of selected publications involving UAH personnel as principal author are attached.

REFERENCES

[1] Fishman, G.J., Meegan, C.A., Wilson, R.B., Brock, M.N., Horack, J.M., Kouveliotou, C., Howard, S., Paciesas, W.S., Briggs, M.S., Pensleton, G.N., Koshut, T.M., Mallozzi, R.S., Stollberg, M., and Lestrade, J.P. "The First BATSE Gamma-Ray Burst Catalog." *Ap. J. Suppl.*, in press (1994).

[2] Kouveliotou, C., Meegan, C.A., Fishman, G.J., Bhat, N.P., Briggs, M.S., Koshut, T.M., Paciesas, W.S., and Pendleton, G.N. "Identification of Two Classes of Gamma-Ray Bursts." *Ap. J.* **413**, L101 (1993).

[3] Koshut, T.M., Pendleton, G.N., Mallozzi, R.S., Paciesas, W.S., and Briggs, M.S. "A Study of Continuum Spectra of Short Duration Gamma-Ray Bursts Observed by BATSE." In *Gamma-Ray Bursts: Huntsville, AL 1993*, ed. G.J. Fishman, J.J. Brainerd and K. Hurley (New York: Am. Inst. Phys.) in press (1994). [See attachment]

[4] Koshut, T.M., Paciesas, W.S., Pendleton, G.N., Brock, M.N., Fishman, G.J., Meegan, C.A., and Wilson, R.B. "An Evaluation of BATSE Burst Locations Computed with the MAXBC Datatype." In *Gamma-Ray Bursts: Huntsville, AL 1993*, ed. G.J. Fishman, J.J. Brainerd and K. Hurley (New York: Am. Inst. Phys.) in press (1994). [See attachment]

[5] Palmer, D.M., Teegarden, B.J., Schaefer, B.E., Cline, T.L., Band, D.L., Ford, L.A., Matteson, J.L., Preece, R.D., Paciesas, W.S., Pendleton, G.N., Briggs, M.S., Fishman, G.J., Meegan, C.A., WIlson, R.B., and Lestrade, J.P. "The Search for Gamma-Ray Burst Spectral Features in the Compton GRO BATSE Data." In *Gamma-Ray Bursts: Huntsville, AL 1993*, ed. G.J. Fishman, J.J. Brainerd and K. Hurley (New York: Am. Inst. Phys.) in press (1994).

[6] Ford, L., Band, D., Matteson, J., Palmer, D., Schaefer, B., Teegarden, B., Preece, R., Briggs, M., Paciesas, W., and Pendleton, G. "A Candidate Absorption Feature from a Gamma Ray Burst Observed by BATSE." In *Gamma-Ray Bursts: Huntsville, AL 1993*, ed. G.J. Fishman, J.J. Brainerd and K. Hurley (New York: Am. Inst. Phys.) in press (1994).

[7] Preece, R.D., Briggs, M., Paciesas, W., Pendleton, G., Ford, L., Band, D., Matteson, J., Palmer, D., Teegarden, B., Schaefer, B., and Brock, M. "Consistency Analysis of a Candidate Line Feature in GRB930506." In *Gamma-Ray Bursts: Huntsville, AL 1993*, ed. G.J. Fishman, J.J. Brainerd and K. Hurley (New York: Am. Inst. Phys.) in press (1994).

[8] Band, D., Ford, L., Matteson, J., Palmer, D., Teegarden, B., Schaefer, B., Briggs, M., Paciesas, W., Pendleton, G., and Preece, R. "Cyclotron Line Search: BATSE-Ginga Consistency." In *Gamma-Ray Bursts: Huntsville, AL 1993*, ed. G.J. Fishman, J.J. Brainerd and K. Hurley (New York: Am. Inst. Phys.) in

press (1994).

[9] Band, D., Ford, L.A., Matteson, J.L., Briggs, M., Paciesas, W., Pendleton, G., Palmer, D., Teegarden, B., Schaefer, B., and Preece, R. "BATSE Line Search: I. Bayesian Consistency Methodology." Submitted to *Ap. J.* (1994).

[10] Schaefer, B.E., Teegarden, B., Palmer, D.M., Cline, T.L., Mitsuka, S., Ford, L.A., Band, D.L., Matteson, J.L., Briggs, M.S., Paciesas, W.S., Pendleton, G.N., and Preece,, R.D. "BATSE Cyclotron Line Search Protocol." In *Gamma-Ray Bursts: Huntsville, AL 1993*, ed. G.J. Fishman, J.J. Brainerd and K. Hurley (New York: Am. Inst. Phys.) in press (1994).

[11] Bhat, N.P., Fishman, G.J., Meegan, C.A., Wilson, R.B., Kouveliotou, C., Paciesas, W.S., Pendleton, G.N., and Schaefer, B.E. "Spectral Evolution of a Sub-Class of Gamma Ray Bursts Observed by BATSE." *Ap. J.*, in press (1994).

[12] Ford, L., Band, D., Matteson, J., Teegarden, B., and Paciesas, W. "Continuum Evolution of Bright Gamma Ray Bursts Observed by BATSE." In *Gamma-Ray Bursts: Huntsville, AL 1993*, ed. G.J. Fishman, J.J. Brainerd and K. Hurley (New York: Am. Inst. Phys.) in press (1994).

[13] Mallozzi, R.S., Pendleton, G.N., Koshut, T.M., Paciesas, W.S., and Briggs, M.S. "The Energy Emission of Gamma-Ray Bursts and Solar Flares." In *Gamma-Ray Bursts: Huntsville, AL 1993*, ed. G.J. Fishman, J.J. Brainerd and K. Hurley (New York: Am. Inst. Phys.) in press (1994). [See attachment]

[14] Preece, R.D., Briggs, M.S., Paciesas, W.S., Pendleton, G.N., Kouveliotou, C., and Brock, M.N. "Spectral Curvature in High-Energy Gamma Ray Bursts Observed by the BATSE Large Area Detectors." In *Gamma-Ray Bursts: Huntsville, AL 1993*, ed. G.J. Fishman, J.J. Brainerd and K. Hurley (New York: Am. Inst. Phys.) in press (1994).

[15] Schaefer, B.E., Teegarden, B.J., Fantasia, S.F., Palmer, D., Cline, T.L., Matteson, J.L., Band, D.L., Ford, L.A., Fishman, G.J., Meegan, C.A., Wilson, R.B., Paciesas, W.S., Pendleton, G.N., Briggs, M.S., and Lestrade, J.P. "BATSE Spectroscopy Catalog of Bright Gamma-Ray Bursts." *Ap. J. Suppl.*, in press (1994).

[16] Pendleton, G.N., Paciesas, W.S., Briggs, M.S., Mallozzi, R.S., Koshut, T.M., Fishman, G.J., Meegan, C.A., Wilson, R.B., Harmon, B.A., and Kouveliotou, C. "The Continuum Spectral Characteristics of Gamma-Ray Bursts Observed by BATSE." *Ap. J.*, in press (1994).

[17] Pendleton, G.N., Paciesas, W.S., Briggs, M.S., Fishman, G.J., Wilson, R.B., Meegan, C.A., and Kouveliotou, C. "Continuum Spectral Characteristics of Bursts Measured with the BATSE Large Area Detectors." In *Gamma-Ray Bursts:*

Huntsville, AL 1993, ed. G.J. Fishman, J.J. Brainerd and K. Hurley (New York: Am. Inst. Phys.) in press (1994). [See attachment]

[18] Fenimore, E.E., Epstein, R.I., Ho, C., Klebesadel, R.W., Lacey, C., Laros, J.G., Meier, M., Strohmayer, T., Pendleton, G., Fishman, G., Kouveliotou, C., and Meegan, C. "The intrinsic luminosity of gamma-ray bursts and their host galaxies." *Nature* **366**, 40 (1993).

[19] Brainerd, J.J., Paciesas, W.S., Meegan, C.A., and Fishman, G.J. "The Nearest Neighbors of BATSE Gamma-Ray Bursts: Narrowing the Possibilities." In *Gamma-Ray Bursts: Huntsville, AL 1993*, ed. G.J. Fishman, J.J. Brainerd and K. Hurley (New York: Am. Inst. Phys.) in press (1994). [See attachment]

[20] Horack, J.M., Koshut, T.M., Mallozzi, R.S., Storey, S.D., and Emslie, A.G. "Implications of the BATSE Data for a Heliocentric Origin of Gamma-Ray Bursts." *Ap. J.*, in press (1994).

[21] Hakkila, J., Meegan, C.A., Pendleton, G.N., Fishman, G.J., Wilson, R.B., Paciesas, W.S., Brock, M.N., and Horack, J.M. "Constraints on Galactic Distributions of Gamma ray Burst Sources from BATSE Observations." *Ap. J.*, **422**, 659 (1994).

[22] Kouveliotou, C., Fishman, G.J., Meegan, C.A., Paciesas, W.S., Wilson, R.B., van Paradijs, J., Preece, R.D., Briggs, M.S., Pendleton, G.N., Brock, M.N., Koshut, T.M., and Horack, J.M. "Recurrent burst activity from the soft gamma-ray repeater SGR 1900+14." *Nature* **362**, 728 (1993).

[23] Kouveliotou, C., Fishman, G.J., Meegan, C.A., Paciesas, W.S., van Paradijs, J., Norris, J.P., Preece, R.D., Briggs, M.S., Horack, J.M., Pendleton, G.N., and Green D.A. "The rarity of soft gamma-ray repeaters deduced from reactivation of SGR 1806-20." *Nature* **368**, 125 (1994).

[24] Kouveliotou, C., Preece, R., Bhat, N., Fishman, G.J., Meegan, C.A., Horack, J.M., Briggs, M.S., Paciesas, W.S., Pendleton, G.N., Band, D., Matteson, J., Palmer, D., Teegarden, B.J., and Norris, J.P. "BATSE Observations of the Very Intense Gamma-Ray Burst GRB 930131." *Ap. J.*, **422**, L59 (1994).

[25] Norris, J.P., Nemiroff, R.J., Scargle, J.D., Kouveliotou, C., Fishman, G.J., Meegan, C.A., Paciesas, W.S., and Bonnell, J.T. "Detection of Signature Consistent with Cosmological Time Dilation in Gamma-Ray Bursts." *Ap. J.*, in press (1994).

[26] Mitrofanov, I.G., Chernenko, A.M., Pozanenko, A.S., Paciesas, W.S., Kouveliotou, C., Meegan, C.A., Fishman, G.J., and Sagdeev, R.Z. In *Gamma-Ray Bursts: Huntsville, AL*

1993, ed. G.J. Fishman, J.J. Brainerd and K. Hurley (New York: Am. Inst. Phys.) in press (1994).

[27] Brainerd, J.J. "Producing the Universal Spectrum of Cosmological Gamma-Ray Bursts with the Klein-Nishina Cross Section." *Ap. J.*, in press (1994).

[28] Brainerd, J.J., "The Compton Attenuation Model of Cosmological Gamma-Ray Bursts." In *Gamma-Ray Bursts: Huntsville, AL 1993*, ed. G.J. Fishman, J.J. Brainerd and K. Hurley (New York: Am. Inst. Phys.) in press (1994). [See attachment]

[29] Brainerd, J.J., "Mimicking the Cosmological Time Dilation of Gamma-Ray Bursts in Euclidian Space." *Ap. J.*, in press (1994).

[30] Mallozzi, R.S., Paciesas, W.S., Pendleton, G.N., Briggs, M.S., Harmon, B.A., Wilson, C.A., and Zhang, S.N. "A Search for Extra-Galactic Source Emission using the Earth Occultation Technique." In *The Second Compton Symposium*, ed. C.E. Fichtel, N. Gehrels and J. P. Norris (New York: Am. Inst. Phys.) in press (1994).

[31] Paciesas, W.S., Mallozzi, R.S., Pendleton, G.N., Harmon, B.A., Wilson, C.A., Zhang, S.N., and Fishman, G.J. "BATSE Observations of 3C 273." In *The Second Compton Symposium*, ed. C.E. Fichtel, N. Gehrels and J. P. Norris (New York: Am. Inst. Phys.) in press (1994).

[32] Paciesas, W.S., Briggs, M.S., Pendleton, G.N., Harmon, B.A., Wilson, C.A., Zhang, S.N., and Fishman, G.J. "BATSE Observations of Nova Muscae 1991." In *The Evolution of X-Ray Binaries*, ed. C. Day and S.S. Holt (New York: Am. Inst. Phys.) in press (1994).

[33] Paciesas, W.S., Pendleton, G.N., Harmon, B.A., Wilson, C.A., and Ling, J.C. To be published in *The Gamma-Ray Sky with Compton/GRO and Sigma*, ed. M. Signore (1994).

[34] Harmon, B.A., Wilson, C.A., Paciesas, W.S., Pendleton, G.N., Briggs, M.S., Rubin, B.C., Finger, M.H., Fishman, G.J., Brock, M.N., Wilson, R.B., and Meegan, C.A. "Observation of GX 339-4 Hard State Outbursts in 1991 and 1992." *Ap. J.*, in press (1994).

[35] Harmon, B.A., Zhang, S.N., Wilson, C.A., Rubin, B.C., Fishman, G.J., and Paciesas, W.S. "BATSE Observations of Transient Hard X-Ray Sources." In *The Second Compton Symposium*, ed. C.E. Fichtel, N. Gehrels and J. P. Norris (New York: Am. Inst. Phys.) in press (1994).

[36] Harmon, B.A., Zhang, S.N., Fishman, G.J., Paciesas, W.S., Rubin, B.C., Meegan, C.A., Wilson, R.B., and Finger, M.H. "BATSE Observations of GX 354-0." In *The Second Compton*

Symposium, ed. C.E. Fichtel, N. Gehrels and J. P. Norris (New York: Am. Inst. Phys.) in press (1994).

[37] Zhang, S.N., Fishman, G.J., Harmon, B.A., and Paciesas, W.S. "Imaging high-energy astrophysical sources using Earth occultation." *Nature* **366**, 245 (1993).

[38] Zhang, S.N., Fishman, G.J., Harmon, B.A., Paciesas, W.S., Rubin, B.A., Meegan, C.A., Wilson, R.B., and Finger, M.H. "BATSE Images of the Galactic Center Region." In *The Second Compton Symposium*, ed. C.E. Fichtel, N. Gehrels and J. P. Norris (New York: Am. Inst. Phys.) in press (1994).

[39] Zhang, S.N., Fishman, G.J., Harmon, B.A., Paciesas, W.S., Meegan, C.A., Wilson, R.B., Finger, M.H., and Rubin, B.C. "A Maskless Gamma-Ray All-Sky Imager: BATSE/CGRO." *IEEE Trans. Nucl. Sci.*, in press (1994).

[40] Greiner, J., Snowden, S., Harmon, B.A., Kouveliotou, C., and Paciesas, W. "ROSAT and BATSE Observations of GRS 1915+105." In *The Second Compton Symposium*, ed. C.E. Fichtel, N. Gehrels and J. P. Norris (New York: Am. Inst. Phys.) in press (1994).

[41] Ling, J.C., Wheaton, W.A., Skelton, R.T., Harmon, B.A., Fishman, G.J., and Paciesas, W.S. "BATSE Observations of Cygnus X-1." In *The Second Compton Symposium*, ed. C.E. Fichtel, N. Gehrels and J. P. Norris (New York: Am. Inst. Phys.) in press (1994).

[42] Stollberg, M.T., Paciesas, W.S., Finger, M.H., Fishman, G.J., Wilson, R.B., Harmon, B.A., and Wilson, C.A. "Recent Observations of EXO 2030+375 with BATSE." In *The Evolution of X-Ray Binaries*, ed. C. Day and S.S. Holt (New York: Am. Inst. Phys.) in press (1994).

[43] Wilson, R.B., Harmon, B.A., Fishman, G.J., Finger, M.H., Stollberg, M.T., Pendleton, G.N., Briggs, M., Prince, T.A., Bildsten, L., Chakrabarty, D., Rubin, B.C., and Zhang, S.N. "BATSE Discovery of a Hard X-Ray Pulsar: GRO J1008-57." In *The Second Compton Symposium*, ed. C.E. Fichtel, N. Gehrels and J. P. Norris (New York: Am. Inst. Phys.) in press (1994).

[44] Wilson, R.B., Harmon, B.A., Fishman, G.J., Finger, M.H., Stollberg, M.T., Pendleton, G.J., Briggs, M., Prince, T., Bildsten, L. Chakrabarty, D., Rubin, B.C., and Zhang, S.N. "Discovery of the Hard X-Ray Pulsar GRO J1008-57 by BATSE." In *The Evolution of X-Ray Binaries*, ed. C. Day and S.S. Holt (New York: Am. Inst. Phys.) in press (1994).

[45] Wilson, R.B., Finger, M.H., Pendleton, G.J., Briggs, M., and Bildsten, L. "BATSE Observations of Her X-1: The 35 Day Cycle, Orbit Determination, and Torque Studies." In *The Second Compton Symposium*, ed. C.E. Fichtel, N. Gehrels and

J. P. Norris (New York: Am. Inst. Phys.) in press (1994).

[46] Wilson, R.B., Finger, M.H., Pendleton, G.N., Briggs, M., and Bildsten, L. "Observations of a Correlation between Main-On Intensity and Spin Behavior in Her X-1." In *The Evolution of X-Ray Binaries*, ed. C. Day and S.S. Holt (New York: Am. Inst. Phys.) in press (1994).

[47] Rubin, B.C., Finger, M.H., Wilson, R.B., Fishman, G.J., Meegan, C.A., Paciesas, W.S., Prince, T., Chiu, J., and Chakrabarty, D. "BATSE Observations of 4U 1538-52: A 530 Second Pulsar." In *The Evolution of X-Ray Binaries*, ed. C. Day and S.S. Holt (New York: Am. Inst. Phys.) in press (1994).

ATTACHMENTS

THE NEAREST NEIGHBORS OF BATSE GAMMA-RAY BURSTS: NARROWING THE POSSIBILITIES

J.J. Brainerd,* W.S. Paciesas
Dept. of Physics, University of Alabama in Huntsville, Huntsville, AL 35899

C.A. Meegan, G.J. Fishman
NASA/Marshall Space Flight Center, ES-66, Huntsville, AL 35812

ABSTRACT

The large errors in the locations of gamma-ray bursts observed by the Bursts and Transient Source Experiment (BATSE) forces one to adopt statistical comparisons of the burst catalog to models of burst isotropy to determine if bursts are repeating or clustered. In the first BATSE catalog[1], a nearest neighbor analysis finds a deviation from isotropy.[2] In a recent article[3] It was shown that known instrumental effects cannot produce significant small scale anisotropies. It was also shown that burst repeater models can produce the observe anisotropies. In this paper we examine in more detail repeater burst models. We also show that nearest and farthest neighbor analyses of more recent bursts fail to find significant small scale clustering.

INTRODUCTION

A nearest neighbor analysis[2] of the first BATSE Gamma-Ray Burst Catalog[1] finds a maximum deviation from the isotropic nearest neighbor cumulative distribution of 2% statistical significance.[3] This contradicts an earlier analysis that examines the average value of the nearest neighbor separation and finds no significant deviation from isotropy.[4] The question arises whether the result of the first named analysis is a consequence of statistical fluctuations or of either instrumental or physical processes. The authors of one article[5] assert that the deviation must be of instrumental origin, because a similar farthest neighbor analysis of the first Catalog finds a maximum deviation from the isotropic cumulative distribution of 11% significance, which they regard as statistically significant and unphysical.

In a recent article[3] it was shown that there are no systematic effects that can produce a deviation of the magnitude seen in the data. The effect of the blockage of the sky by the earth produces a maximum deviation of $D = 0.006$ from the isotropic cumulative distribution, which is much smaller than the $D = 0.12$ deviation of the First Catalog. While one might expect a small angle anisotropy from the flux dependence of the sky map to introduce a deviation, we find from Monte Carlo simulation that the maximum deviation from the isotropic cumulative distribution is $D = 0.01$ without any spacecraft reorientations and $< 10^{-3}$ with the reorientations experienced by the Compton Gamma-Ray Observatory (CGRO). Moreover, performing the nearest and farthest neighbor analyses in the spacecraft coordinate frame produces maximum

* Mailing Address: Space Science Lab, ES-66, NASA/MSFC, Huntsville, AL 35812. E-mail: brainerd@ssl.msfc.nasa.gov

deviations of $\approx 50\%$ significance. If the deviation in the First Catalog is non-statistical, it must have a physical origin.

The suggestion of Lamb and Quashnock[2] that repeating burst sources are responsible for the nearest neighbor results is not invalidated by the farthest neighbor analysis.[3] In fact, if repeating burst sources are confined to the galactic plane, the resulting nearest and farthest neighbor distributions agree with the First Catalog distributions without violating the limits on the dipole and quadrupole moments.

In this paper we discuss disk confined repeater models in more detail, presenting their nearest and farthest neighbor cumulative distributions. We also present nearest and farthest neighbor analyses of a recent set of 260 gamma-ray bursts; the results are consistent with an isotropic distribution of bursts.

BURST MODELS

The nearest neighbor of a given burst is primarily determined by the local density of bursts on the sky. The magnitude of the density fluctuations therefore determines the shape of the cumulative distribution. On the other hand, both the magnitude and topology of density fluctuations strongly affect the farthest neighbor cumulative distribution. This implies that the farthest neighbor distribution is much more model dependent than the nearest neighbor distribution.

Two simple models illustrates this point. First, imagine that αN bursts are distributed on the upper celestial hemisphere and $(1-\alpha)N$ bursts are distributed in the lower celestial hemisphere, where N, the total number of bursts, is very large. The nearest neighbor distribution is then

$$F_n = \alpha \exp\left(-\frac{1-\cos\theta}{4N\alpha}\right) + (1-\alpha)\exp\left(-\frac{1-\cos\theta}{4N(1-\alpha)}\right), \qquad (1)$$

and the farthest neighbor distribution is

$$F_f = (1-\alpha)\exp\left(-\frac{1-\cos\theta}{4N\alpha}\right) + \alpha \exp\left(-\frac{1-\cos\theta}{4N(1-\alpha)}\right). \qquad (2)$$

The isotropic nearest and farthest cumulative distributions ($\alpha = 1/2$) equal $1/2$ when $1-\cos\theta = 2N\ln 2$. For this value, $F_n > 1/2$ and $F_f < 1/2$ for all $\alpha \neq 1/2$. Now consider a second model in which $\alpha N/2$ bursts are distributed on one half of the upper hemisphere and the same number of bursts are distributed on the geometrically opposed half of the lower hemisphere. The remaining two half-hemispheres have $(1-\alpha)N/2$ bursts apiece. In this model the nearest and farthest cumulative distributions are both given by equation (1), proving the importance of the topology of density variations.

These simple models illustrate a second point: the nearest neighbor cumulative distribution lies above the isotropic distribution for small vales of $1-\cos\theta$, but the farthest neighbor distribution can lie on either side of the isotropic distribution. However, the magnitude of the deviation from isotropy of the nearest neighbor distribution also depends on the density gradient, for α must be less than ≈ 0.15 to produce a deviation as large as in the left hand plot of Figure 1. This effect disappears as N increases.

The source of the anisotropy also determines whether the deviation of the cumulative distribution from the isotropy distribution changes as the number

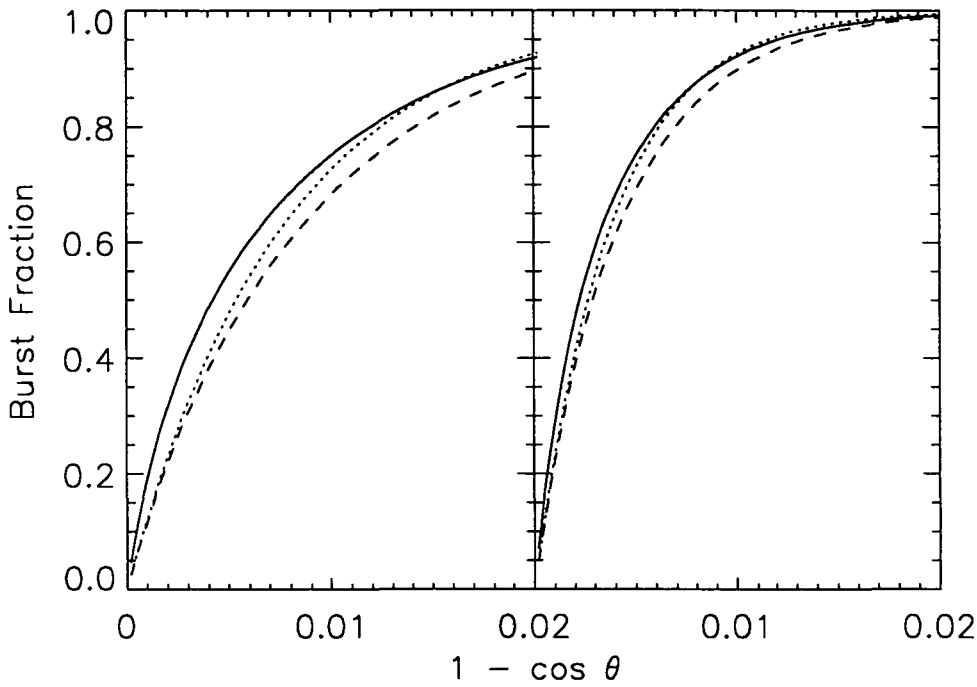

Figure 1. The nearest and farthest neighbor cumulative distributions: effect of sample size. Theoretical curves for a model in which burst sources are isotropically distributed and a fraction of the burst sources producing 4 bursts apiece. The isotropic cumulative distribution is given by the dotted line, the model nearest neighbor distribution by the solid line, and the model farthest neighbor distribution by the dashed line. Left: 200 single burst sources and 15 multiple burst sources. Right: 400 single burst sources and 30 multiple burst sources.

of bursts increases. If the anisotropy arises from the presence of a disk component, then the anisotropy persists. If repeating sources produce the anisotropy through local density enhancements over a location error angular scale, then the cumulative distributions should go to the isotropic distribution as the number of bursts increases beyond the point where the location errors about each repeating source overlaps with adjacent repeating sources. Figure 1 demonstrates the dependence of the cumulative distribution on the sample size. As a consequence, a statistical search for repeaters should use consecutive sets of bursts with a fixed number of bursts in each set.

Figure 1 shows that isotropically distributed repeating sources produce a farthest neighbor cumulative distribution that falls below the isotropic distribution. If the repeaters are confined to the galactic plane, as in Figure 2, the farthest neighbor cumulative distribution can fall above the isotropic distribution.

The model used in Figure 2 has two components, with one component an isotropically distributed set of single burst sources and the second component a set of multiply bursting sources confined to the galactic plane. Such models can reproduce the nearest neighbor distribution of the First BATSE Catalog

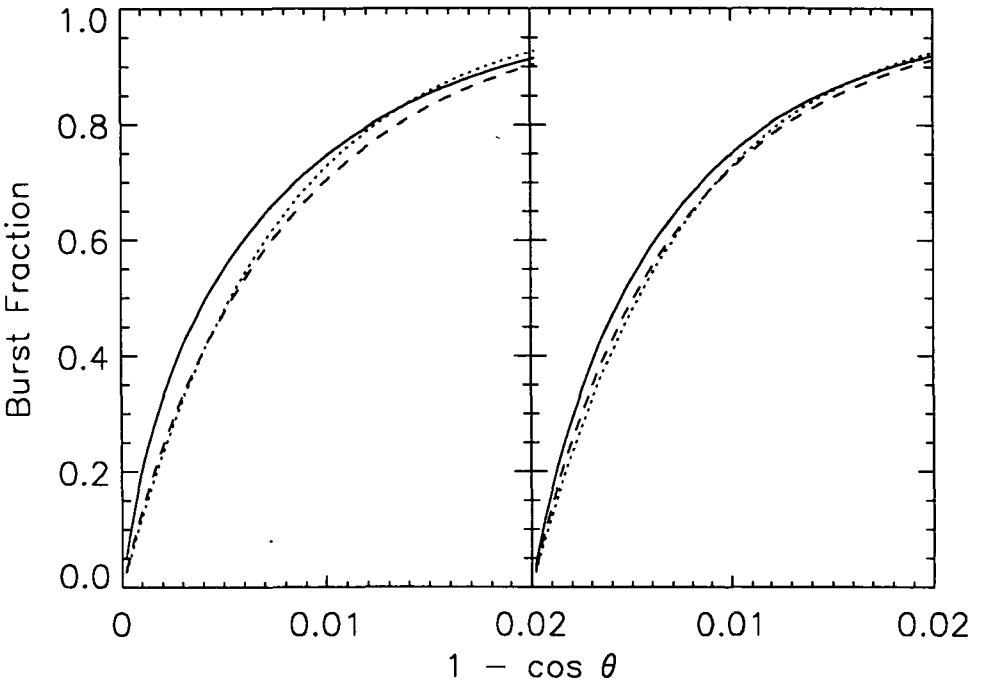

Figure 2. The nearest and farthest neighbor cumulative distributions: quadruple repeaters versus double repeaters. Two hundred single burst sources are isotropically distributed. Additional repeating sources are uniformly distributed between $\pm 10°$ galactic latitude. The position of each outburst relative to the source is given by a gaussian distribution function with average offset of 5°. The lines are defined as in Fig. 1. Left: 15 repeating sources burst 4 times apiece. Right: 30 repeating sources burst 2 times apiece.

without violating constraints on the farthest neighbor distribution or the value of $\langle \sin^2 b \rangle$. The right hand plot of Figure 2 deviates from the the observed nearest and farthest neighbor distributions with significances of 68% and 31% respectively. In this model one finds $\sin^2 b = 0.26$, which is less than 3σ from the value in the First Catalog.

RECENT RESULTS AND CONCLUSIONS

The Kolmogorov-Smirnov statistic for the nearest neighbor distribution from the First BATSE Catalog[3] of 260 bursts is $N^{1/2}D = 1.86$, which has a 2% significance. A farthest neighbor analysis gives $N^{1/2}D = 1.56$, which has an 11% significance.[5] These values are consistent with both a statistical origin and a physical origin.

A more recent ensemble of 260 gamma-ray bursts disjoint from the first catalog shows no evidence for anisotropy. Their nearest and farthest neighbor cumulative distributions are given in figure 3. The maximum deviation of the nearest neighbor cumulative distribution is below the isotropic cumulative dis-

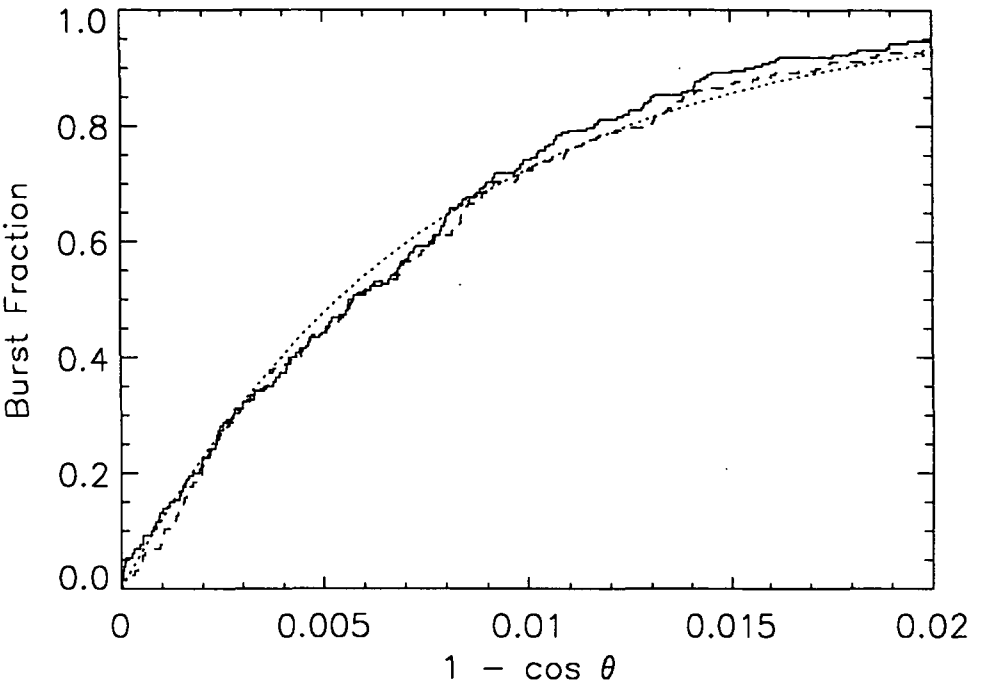

Figure 3. The nearest and farthest neighbor cumulative distributions: recent gamma-ray burst sample. A set of 260 gamma-ray bursts is selective by dropping all gamma-ray bursts with locations by the BATSE data type MAX-BC from the set of triggers between 1819 and 2494 inclusive (GRB920814b to GRB930817). These bursts will be part of the 2B and 3B gamma-ray burst catalogs. The lines are defined as in Fig. 1.

tribution, and gives $N^{1/2}D = 0.77$, with significance 83%. The farthest neighbor distribution has $N^{1/2}D = 0.85$, with significance 75%. Again the maximum deviation is below the isotropic cumulative distribution. This provides no support for the belief that the deviation found in the first catalog has a physical origin.

REFERENCES

1. G.J. Fishman, C.A. Meegan, R.B. Wilson, M.N. Brock, J.M. Horack, C. Kouveliotou, S. Howard, W.S. Paciesas, M.S. Briggs, G.N. Pendleton, T.M. Koshut, R.S. Mallozzi, M. Stollberg & P. Lestrade, Astrophys. J. Suppl. Ser., in press, (1994).
2. Quashnock & D.Q. Lamb, Mon. Not. R. Astron. Soc., in press, (1993).
3. J.J. Brainerd, Astrophys. J. Lett., submitted, (1994).
4. J.M. Horack, G.J. Fishman, C.A. Meegan, R.B. Wilson, M.N. Brock, J. Hakkila, W.S. Paciesas, G.N. Pendleton, & M.S. Briggs, in *Compton Gamma-Ray Observatory: St. Louis, MO 1992*, ed. M. Friedlander, N. Gehrels, & D.J. Macomb (AIP: New York, 1993), p. 699.
5. Narayan & T. Piran, Mon. Not. R. Astron. Soc., in press, (1993).

THE COMPTON ATTENUATION MODEL OF COSMOLOGICAL GAMMA-RAY BURSTS

J.J. Brainerd*
Dept. of Physics, University of Alabama in Huntsville

ABSTRACT

A gamma-ray burst spectrum can be modeled by passing a power law spectrum through a medium that is optically thick to Compton scattering. The roll-over of the Klein-Nishina cross section at high energies produces a break in the spectrum at several hundred keV if the gamma-ray source is at $z \approx 1$. Photon-photon pair production limits the scattering region's size to greater than ≈ 0.1 parsec. Because the optical depth is greater than unity for a length scale of several parsecs, the density must be of order $10^5 \mathrm{cm}^{-3}$, which occurs only in molecular clouds at the centers of galaxies. This model therefore precludes source models employing objects that are common to the galactic plane—for example, merging neutron stars. The model spectrum is described by five free parameters: a cosmological red shift, a Thomson optical depth, a power law index, a metallicity, and an amplitude. The attenuation model can be tested by comparing the consistency of model parameters derived at different times over the duration of a burst. Small angle scattering of x-rays by dust within the molecular cloud produces an x-ray afterglow. A consequence of this model is that any optical or ultraviolet radiation is heavily absorbed, making detection of gamma-ray bursts at these energies unlikely.

INTRODUCTION

A long standing problem in constructing models of gamma-ray bursts is modeling the non-thermal burst spectrum. These spectra are generally a power law above 1MeV, and emit their peak power at several hundred keV.[1,2] Before BATSE, when the predominate models were emission from neutron stars, the small fraction of energy in the x-ray band caused considerable theoretical difficulty, and became known as the x-ray paucity problem. Now we have cosmological models which have no predefined characteristic energy, implying that the characteristic spectral energy peak is still a problem.

The root of the difficulty with cosmological models is the large Lorentz factors of $\gamma > 100$ required to overcome photon-photon pair creation. This makes the characteristic energy in the rest frame of the emitter ill-defined, because the value of the Lorentz factor is not physically constrained. The likely radiative processes—photoelectric absorption, cyclotron emission, Compton scattering—are further unconstrained in optical depth, electron distribution, magnetic field strength, and seed photon density and energy.

These considerations suggest that the characteristic energy of gamma-ray bursts is set by processes in the rest frame of the host galaxy and is associated with the electron rest mass energy. This article examines Compton attenuation as the mechanism responsible for producing the observed spectra. More detailed

* Mailing Address: Space Science Lab, ES-66, NASA/MSFC, Huntsville, AL 35812. E-mail: brainerd@ssl.msfc.nasa.gov

analyses of this model are presented elsewhere.[3,4]

THE COMPTON ATTENUATION MODEL

Because the purpose of this model is to explain the characteristic peak values of the νF_ν curve independent of the Lorentz factor of the source, I must assume that the source spectrum is a power law. In the model the source is embedded in a cool, static medium with Thomson optical depth much greater than unity. Compton scattered radiation can annihilate with other burst photons and produce electron-positron pairs. If significant scattering occurs closer than $\approx d_s = 0.04\,(\tau/10)\exp(\tau/2-5)$ pc to the source, where τ is the Thomson optical depth of the scattering region, the number of pairs created raises the optical depth by at least 1, which produces a rapid and permanent extinction of the gamma-ray burst. As this contradicts the observations, the scattering region must be larger than d_s. The travel time between scatterings is therefore $> 10^6$s, so the scattered radiation does not contribute to the burst.

A second process affects the x-ray spectrum: photoelectric absorption. Because the scattering region is primarily composed of hydrogen, this process affects the spectrum at the lower energy limit of the BATSE instrument (approximately 20keV). The energy of unity optical depth is pushed far below the instrument threshold for a cosmological red shift of $z \approx 1$. As a consequence, photoelectric absorption is generally unimportant for fitting the spectra of bursts observed by BATSE.

Figure 1 shows the Compton attenuated spectrum for several values of the Thomson optical depth. At high energies the scattering optical depth falls to zero because of the ν^{-1} dependence of the Klein-Nishina cross section above 1MeV. The transition from the Thomson cross section to the Klein-Nishina cross section produces a "broken" spectrum below 1MeV. Below 10keV the effects of photoelectric absorption appear. In the absence of photoelectric absorption the spectrum follows a power law with the index of the source power law spectrum.

The high Thomson optical depth in this model limits it to sources at the centers of galaxies. Because the scattering region is large, it must be associated with the interstellar medium. But the optical depth through the plane of nearby spiral galaxies is much less than unity. This leaves molecular clouds with densities of order $10^5\mathrm{cm}^{-3}$, which exist only at the centers of galaxies. This model is therefore inconsistent with sources common to the planes of galaxies, such as merging binary stars. The source must in fact be unique to the cores of galaxies, which suggests that the energy source in this model is a massive black hole.

X-RAY AFTERGLOW

A small number of bursts have x-ray emission lasting up to several hundred seconds after the gamma-ray emission falls below background.[5,6,7] The afterglow spectrum falls rapidly and can be fit by a black body continuum with a temperature of approximately 1keV to 2keV. To this point the only interpretation offered for this radiation is thermal emission from the burst source. For extragalactic sources this implies a source size of $\approx 10^{10}$cm for $\gamma = 1$, which is larger than the size derived from the rise time.

Because the Compton attenuation model requires a dense molecular cloud for the scattering region, it provides a natural explanation for the x-ray afterglow—coherent scattering with dust.[4,8,9,10] X-rays produced in the gamma-ray

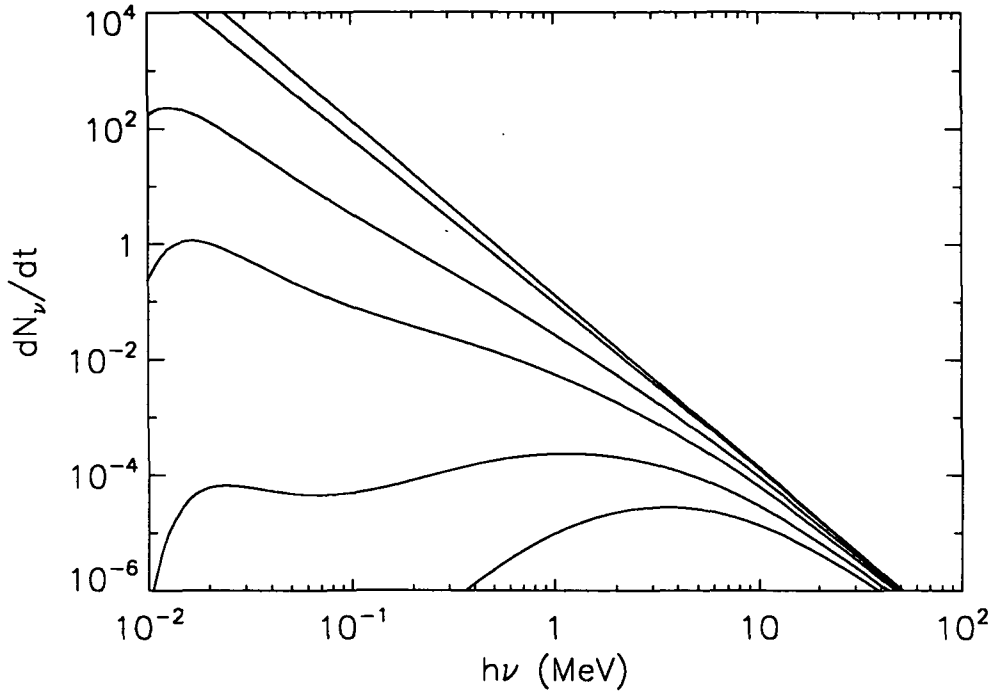

Figure 1. Spectra produced by Compton attenuation of a power law with index $\delta = -3$. The scattering region has 0.5 of the solar abundance of metals. The Thomson optical depths from top to bottom are $\tau = 0$, 1, 5, 10, 20, and 30. No cosmological red shift is present.

burst are scattered by a small angle into the observer's line of sight. The longer propagation path introduces a delay in the x-ray emission relative to the gamma-ray emission. At several keV the scattering angle is of order 10^{-4} radian for a dust particle diameter of 0.01μm, which produces a time delay of 100 seconds if the scattering occurs 10pc from the x-ray source.

I assume the distribution function for dust grain size is

$$f(a) = \frac{3(4-m)\,\rho_m}{4\pi a_0^4 \rho_g} \left(\frac{a_0}{a}\right)^m , \qquad (1)$$

where $a < a_0$ is the grain radius, ρ_g is the mass density within each grain, and ρ_m is the mass density of metals in the molecular cloud. The distribution function is zero when $a \geq a_0$. The total cross section for coherent scattering of x-rays by dust is then[4]

$$\alpha_d = 6.7 \times 10^4 \left(\frac{Z}{A}\right)^2 \frac{4-m}{5-m}\, a_{0\mu m} \rho_m\, \rho_g \left[\frac{F(E)}{Z}\right]^2 E_{keV}^{-2}\ \mathrm{cm}^{-1} . \qquad (2)$$

In this equation the function in brackets is of order unity. For the molecular clouds under consideration in this model, one expects the energy of unity optical depth to be near 10keV. For these equations and the differential scattering cross section, I ran a Monte Carlo simulation of 10^5 photons to produce Figure 2.

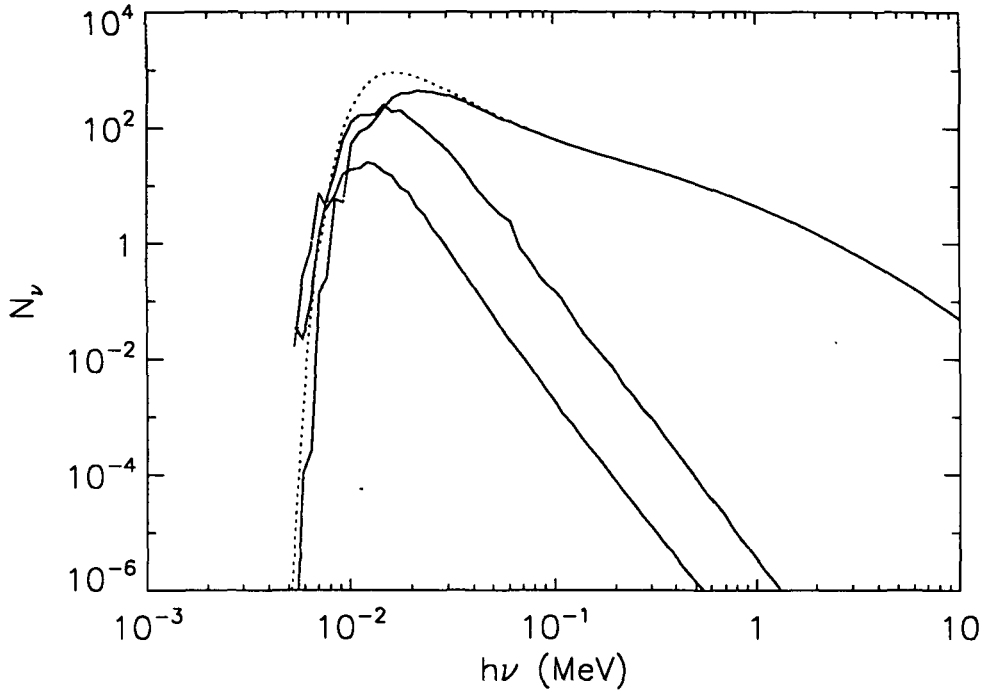

Figure 2. X-Ray afterglow. The dotted curve gives the Compton attenuated burst spectrum in the absence of dust for $\tau = 10$. The remaining parameters are those for Fig. 1. The uppermost solid curve gives the direct spectrum in the presence of dust, where all metals are assumed to be in dust. The dust distribution is given in the text. The remaining two solid curves give the delayed x-ray spectrum. The upper curve is the delayed emission integrated over time 100 s after the burst. The lower curve is the emission integrated between 100 s and 10^3 s.

The dust decreases the direct x-ray flux by a significant factor below 30keV. The afterglow spectrum is quite steep above unity optical depth, having a spectrum given by the burst spectrum times E_{keV}^{7-m}. At low energies the optical depth to scattering exceeds unity, causing the delayed spectrum to be flat. While the spectra in Figure 2 resemble thermal spectra with temperatures of $\approx$ 5keV, which is higher than observed, dust scattered spectra at a cosmological red shift of ≈ 2 will have the correct shape to fit the observations. One characteristic of this model is that the peak of the x-ray afterglow should shift down in energy with time.

OBSERVATIONAL TESTS

The Compton attenuation theory must satisfy a stringent test: model fits to a burst's spectrum at different times over the duration of the burst must yield the same cosmological red shift z. One does not generally expect other models to produce a constant value of z. For instance, if the energy of the spectral break is dependent on the Lorentz factor γ of the emitter, and if γ decreases

with time, the spectral break energy should fall with time, leading to a z that rises with time. The constancy of z with time can also be tested by fitting the color-color diagrams of individual bursts[11] with model color-color curves found by allowing the power law index to vary.

A second test of this model is the comparison of the values of z derived from spectral fits with the allowed values of z implied by each burst's position on the $\log N$–$\log P_{max}$ curve. High values of z must correspond to low values of P_{max}.

The effects of dust offer additional opportunities for testing this theory. The spectrum and time profile of the x-ray afterglow is dependent to some extent on the spectrum and time profile of the direct gamma-ray burst. One should be able to model this correlation and test for its presence. A second test is the presence of an optical flash at the time of the gamma-ray burst. Optical emission during the gamma-ray burst will be heavily absorbed by the dust, making the observation of gamma-ray bursts at these wavelengths unlikely. The observation of an optical flash would pose great physical difficulties for the Compton attenuation model.

REFERENCES

1. D. Band, J. Matteson, L. Ford, B. Schaefer, D. Palmer, B. Teegarden, T. Cline, M. Briggs, W. Paciesas, G. Pendleton, G. Fishman, C. Kouveliotou, C. Meegan, R. Wilson, & P. Lestrade, Astrophys. J. **413**, 281 (1993).
2. C. Winkler, K. Bennett, L. Hanlon, O.R. Williams, W. Collmar, R. Diehl, V. Schönfelder, H. Steinle, M. Varendorff, J.W. den Herden, W. Hermsen, L. Huiper, B.N. Swanenburg, C. de Vries, A. Connors, D. Forrest, M. Kippen, M. McConnell, & J. Ryan, in *Compton Gamma-Ray Observatory: St. Louis, MO 1992*, ed. M. Friedlander, N. Gehrels, & D.J. Macomb (AIP: New York, 1993), p. 845.
3. J.J. Brainerd, Astrophys. J., in press, (1994).
4. J.J. Brainerd, Astrophys. J. Lett., submitted, (1994).
5. J.G. Laros, *et al.*, Astron. Astrophys. **286**, 681 (1982).
6. M. Katoh, T. Murakami, J. Nishimura, T. Yamagami, M., Fujii, & M. Itoh, in *High Energy Transients in Astrophysics*, ed. S.E. Woosley (AIP: New York, 1984), p. 390.
7. T. Murakami, H. Inoue, J. van Paradijs, E.E., Fenimore, & A. Yoshida, in *Gamma-Ray Bursts: Observations, Analyses and Theories*, ed. C. Ho, R.I. Epstein, & E.E. Fenimore (Cambridge University Press: Cambridge, 1992), p. 239.
8. J.W. Overbeck, Astrophys. J. **141**, 864 (1965).
9. C.W. Mauche & P. Gorenstein, Astrophys. J. **302**, 371 (1986).
10. C.S.R. Day & A.F. Tennant, Mon. Not. R. Astron. Soc. **251**, 76 (1991).
11. C. Kouveliotou, W.S. Paciesas, G.J. Fishman, C.A. Meegan, & R.B. Wilson, Astron. Astrophys. **97**, 55 (1993).

A STUDY OF CONTINUUM SPECTRA OF SHORT-DURATION GAMMA-RAY BURSTS OBSERVED BY BATSE

T. M. Koshut, G. N. Pendleton, R. S. Mallozzi, W. S. Paciesas, M. S. Briggs
Dept. of Physics, University of Alabama in Huntsville, Huntsville, AL 35899

ABSTRACT

We use 4 and 16 channel data from the BATSE Large Area Detectors to compare the continuum spectral characteristics of the short-duration bursts with those of short spikes within long-duration bursts. We compare frequency distributions of the resulting best-fit model parameters for the short bursts and for the short spikes within the long bursts. These distributions are different for the two types of events. The best-fit model parameters are used to calculate the peak energy $E_{\rm max}$ of the ν F_ν spectrum for each type of event. The resulting distributions of $E_{\rm max}$ are consistent within a cosmological scenario if the redshift of the short spikes within long-duration bursts is larger than the redshift of the short bursts.

INTRODUCTION

The existence of two subclasses of classical gamma-ray bursts, defined by durations $\leq$ 2.5 seconds and durations $>$ 2.5 seconds (see reference 1, and references therein), has been confirmed.[2] The time histories of the long-duration events often contain substructures with pulse widths that are very similar to the durations of the short-duration bursts. These time histories can be very diverse, ranging from those that are highly variable over the duration of the burst to those having an impulsive spike riding on top of gradually-varying emission. By treating each such substructure as a separate event, we hope to investigate the possibility that each substructure is a manifestation of the same emission mechanism producing the short-duration bursts.

METHODOLOGY

BATSE consists of eight uncollimated Large Area Detectors (LADs), spanning an energy range of $\sim$ 20–2000 keV. Details of BATSE instrumentation can be found elsewhere.[3] Five BATSE data-types are used in this study: Medium Energy Resolution (MER), Discriminator Science (DISCSC), Preburst (PREB), Continuous (CONT), and LAD Discriminator (DISCLA). MER data consist of count rates in 16 energy channels, with a time resolution of 16 ms for the first $\sim$ 32 seconds after the burst trigger time t_o, changing to a time resolution of 64 ms for the next $\sim$ 128 seconds. MER data begins to accumulate $\sim$ 30 ms after t_o, usually making it unsuitable to study the short-duration bursts (which are often over by t_o). The PREB and DISCSC data consist of count rates in 4 energy channels, with a time resolution of 64 ms, starting $\sim$ 2 seconds prior to t_o and lasting until $\sim$ 240 seconds after t_o. CONT data consist of count rates in 16 energy channels, with a time resolution of 2.048 seconds. DISCLA data consist of count rates in 4 energy channels with a time resolution of 1.024 seconds. CONT and DISCLA data are only used for the purpose of background subtraction in this study. Only the 16-channel data were corrected for dead-time effects; the

4-channel data would not have suffered any significant dead-time during the bursts used in this study.

A total of 29 short-duration bursts and 13 long-duration bursts were examined in this study. A count spectrum was integrated over the duration of each short-duration burst. Additionally, within each long-duration burst, a spectrum was integrated over short spikes with a pulse width less than 2.5 seconds. This criterion resulted in 55 short spikes among the long-duration events.

The count spectra were deconvolved to produce photon spectra using a forward-folding model-fitting technique. A detector response matrix was used for each burst, correcting for the detector's energy response function, angular response function, and for flux scattered by the Earth's atmosphere and the CGRO spacecraft.[4] The photon spectrum model employed in the fit was a Gaussian as a function of $\log_{10}(E)$, given by

$$\frac{dN}{dE} = \frac{A}{\sqrt{2\pi}\sigma_g} \exp\left\{-\frac{1}{2}\left[\frac{\log_{10}(E) - \log_{10}(E_{cent})}{\sigma_g}\right]^2\right\} \quad (1)$$

where σ_g is defined as

$$\sigma_g = \frac{\log_{10}(FWHM)}{2.35482} \quad (2)$$

Three parameters were allowed to vary in this model: A, E_{cent}, and σ_g. A represents the amplitude of the Gaussian, E_{cent} is the center of the Gaussian, and σ_g measures its full-width at half-maximum. Though this model is unphysical, it served as a good functional representation for most of the spectra analyzed, making it useful for comparison purposes. The reduced χ^2 for the model-fits to the 4-channel data was, on average, higher than that for the 16-channel data; this is attributed to systematic errors. The uncertainties in the two parameters of interest, E_{cent} and σ_g, were estimated *jointly* by assuming a 68% confidence region in the shape of an ellipsoid, centered on the measured values.[5]

To address the issue of consistency of results using different datatypes we analyzed both 4-channel and 16-channel spectra integrated over the same time intervals for a small sample of bursts. In general, the best-fit parameters agreed within their uncertainties. The amplitude of the 16-channel data was usually slightly larger than that of the 4-channel data, which we attribute to slightly over-correcting the 16-channel data for dead-time effects.

RESULTS

Figure 1a shows a plot of σ_g vs E_{cent} for the set of 29 short bursts. Figure 1b shows the same information for the 55 short spikes within the 13 long-duration bursts. Though it is difficult to draw conclusions from such crowded plots, it does seem clear that there is a large concentration of short spikes within long-duration bursts at low values of E_{cent}. The frequency distributions of E_{cent} and σ_g are given in Figures 2a and 2b, respectively. The distributions for the short-duration bursts are shown as solid lines, while the long-duration bursts are represented by dotted lines. Assuming normally distributed errors, the uncertainties for each bin are simply the square-root of the number of events in that bin.

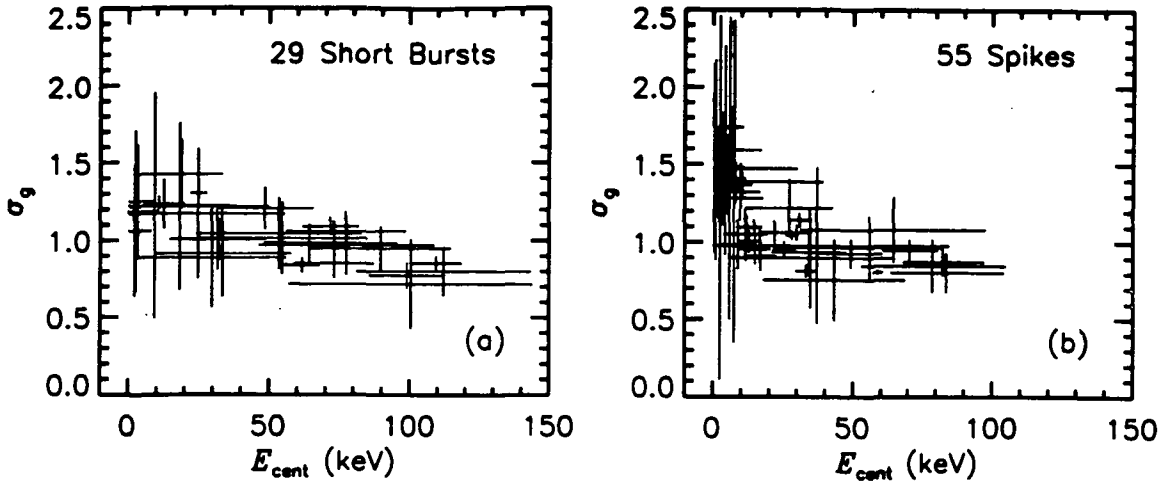

Fig. 1 (a and b). 1a shows a plot of the best-fit model parameters, along with their uncertainties, for the short-duration bursts. 1b shows the same information for the short spikes within the long-duration bursts.

Figure 2a shows that the short spikes within the long-duration bursts and the short-duration bursts sample the same range of parameter space of E_{cent}. However, their distributions are clearly different; i.e., the short spikes in long-duration bursts tend to concentrate at low values of E_{cent} while the values for the short bursts seem to be distributed uniformly over the entire range. This is in contrast to the result of comparing the distributions of σ_g for each type of event, shown in Figure 2b. It indicates that the short bursts do not sample the same range of available parameter space as the short spikes, and moreover, that the range of values of σ_g for the short bursts is a subset of those sampled by the short spikes. Further, there is a hint of a bimodality in the distribution of σ_g in Figure 2b for the short spikes, thus suggesting the interesting possibility of two classes of short spikes within long-duration bursts, based on spectral parameters alone. At this point, no work has been done to identify which long-duration bursts would makeup the two populations shown in Figure 2b, nor has any

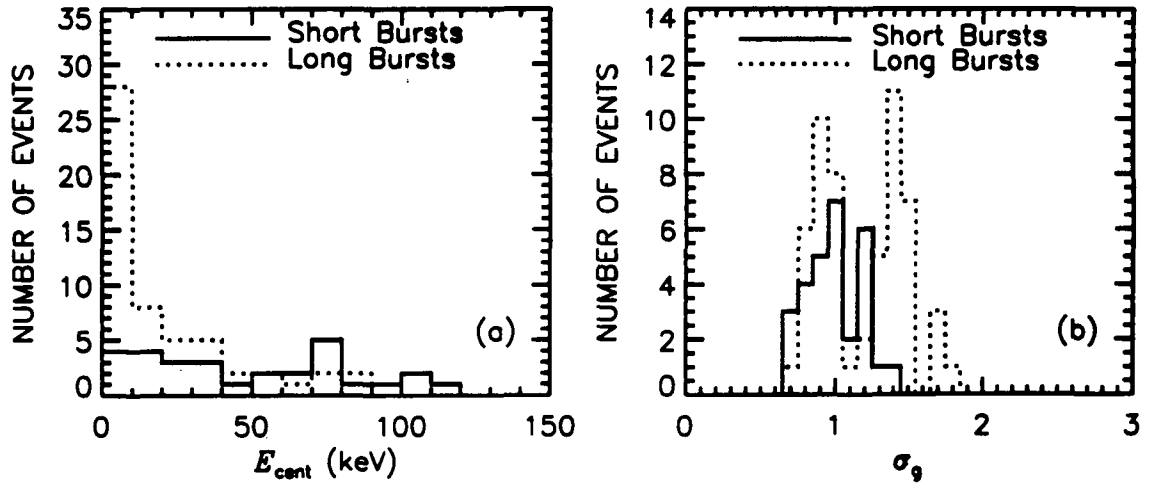

Fig. 2 (a and b). 2a and 2b show the frequency distributions of E_{max} and σ_g, respectively.

attempt been made to correlate σ_g with any other properties (peak intensity, duration, sky distribution, etc.) of the spikes or their "parent" bursts.

It was found that the three freely varying parameters of the function used to model the photon spectrum are significantly correlated. Therefore it is not appropriate to independently use any one of these parameters to characterize a spectrum. To reduce the impact of this correlation, the energy at which the ν F_ν spectrum is a maximum, E_{max}, was calculated analytically for each burst. This is done by multiplying Equation 1 by a factor of E^2 and setting the derivative of the result with respect to E equal to zero. Solving for E_{max} gives

$$\log_{10}(E_{\rm max}) = \log_{10}(E_{\rm cent}) + \frac{2{\sigma_g}^2}{\log_{10}(e)} \qquad (3)$$

$E_{\rm max}$ is then used to characterize each spectrum, with the hope that the effect of the correlation between the parameters has been minimized.

The resulting distributions of $E_{\rm max}$ for the two types of bursts are similar and are shown in Figure 3. The mean value of $E_{\rm max}$ for the short bursts is 394 keV while for the short spikes within the long bursts it is 292 keV. This is consistent with the previously-known result that the short bursts tend to be harder than the long bursts.[2] The uncertainties for each bin in Figure 3 may be approximated as the square-root of the number of events in that bin, assuming that the errors in $E_{\rm max}$ are distributed normally. The uncertainty in $E_{\rm max}$ was calculated in a standard fashion.[6] Assuming that the errors in $E_{\rm cent}$ and σ_g are small, the uncertainty in $E_{\rm max}$ was found using

$$(\delta E_{\rm max})^2 = \left(\frac{\partial E_{\rm max}}{\partial E_{\rm cent}} \frac{\partial E_{\rm max}}{\partial \sigma_g}\right) \begin{pmatrix} (\delta E_{\rm cent})^2 & {\rm cov}(\delta E_{\rm cent}, \delta\sigma_g) \\ {\rm cov}(\delta\sigma_g, \delta E_{\rm cent}) & (\delta\sigma_g)^2 \end{pmatrix} \begin{pmatrix} \frac{\partial E_{\rm max}}{\partial E_{\rm cent}} \\ \frac{\partial E_{\rm max}}{\partial \sigma_g} \end{pmatrix} \qquad (4)$$

where $\delta E_{\rm cent}$ and $\delta\sigma_g$ are the uncertainties in $E_{\rm cent}$ and σ_g, respectively, and the partial derivatives of $E_{\rm max}$ are calculated using Equation 3. The relative errors were usually in the 5–30% range. The uncertainties in $E_{\rm max}$ were often at, or smaller than, the energy resolution of the data. Therefore we do not expect the uncertainties in $E_{\rm max}$ to significantly change the results shown in Figure 3.

With a few simple assumptions, the results shown in Figure 3 may provide some physical insight into the spatial distribution of burst sources. Let us assume that burst sources are at cosmological distances and that the mechanism producing the short-duration bursts is the same mechanism that produces the short spikes within the long-duration

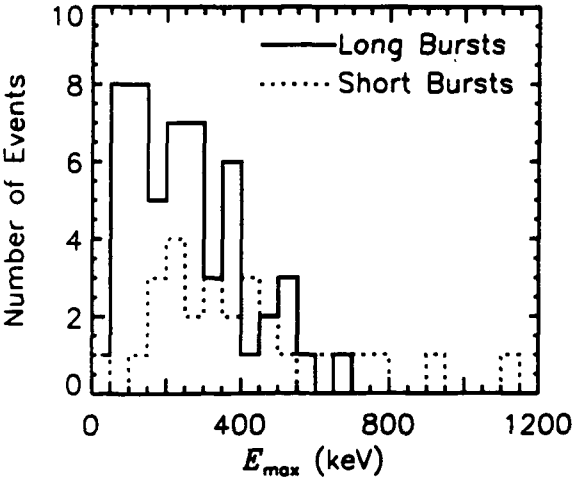

Fig 3. Frequency distributions of $E_{\rm max}$

bursts. By using the mean peak energy of the νF_ν spectrum for each distribution as a characteristic energy, we have calculated the cosmological redshift of the long-duration bursts z_L relative to the redshift of the short-duration bursts z_S. We find that under these assumptions $z_L = 1.35 z_S$. However, a cosmological interpretation is not *required* to explain Figure 3; the fact that short bursts tend to be harder than long bursts, convolved with any tendency for hard-to-soft spectral evolution, would give the same results.

A cautious approach must be taken in interpreting Figures 2 and 3 due to the low statistical significance of the data. The uncertainties in the best-fit parameters may not be normally distributed; thus, the errors on the frequency distributions should be calculated directly from the best-fit parameter uncertainties. It is clear that the uncertainties by themselves will not be able to wash out the strongly peaked distribution of $E_{\rm cent}$ for the short spikes within long-duration bursts shown in Figure 2a. However, the bimodal distribution of σ_g must not be taken too seriously until the uncertainties are more closely examined. Also, it should be pointed out that Equation 4, used to calculate $\delta E_{\rm max}$, breaks down when the uncertainties $\delta E_{\rm cent}$ or $\delta \sigma_g$ are large because second-order terms in the Taylor expansion have been neglected.

FUTURE WORK

There are a number of ways to improve the procedure used in this study. An attempt to choose a larger sample of bursts will be made, allowing more confidence in the interpretation of any interesting results. A function must be chosen for the photon spectrum model in which the freely varying parameters are less correlated. The limitation here is that the only BATSE data types available to study the short-bursts often consist of 4-channel energy spectra; thus the model must contain no more than 3 free parameters to ensure at least one degree-of-freedom in the fitting procedure. It may be possible to use a more complicated model with one parameter fixed to a value that is fairly representative of most of the bursts being studied. Additionally, the assumption of a symmetrical ellipse for the shape of the 68% confidence region when determining the uncertainties in the best-fit parameters may not be accurate. Software to examine these regions for each fit is in place and will be utilized in the future. Finally, the uncertainties in the best-fit parameters should be propagated through the frequency distributions in a more rigorous way. This will indicate how serious one can take features such as the bimodality in Figure 2b.

REFERENCES

1. K. Hurley, in Gamma-Ray Bursts, p. 3, (Huntsville, AIP), (1991)
2. C. Kouveliotou et al., Ap. JLett **413**, L101 (1993)
3. G. Fishman et al., in Proceedings of the GRO Science Workshop, 2-39 (1989)
4. G. Pendleton et al., in Proceedings of the GRO Science Workshop, 4-547 (1989)
5. W. Press, B. Flannery, S. Teukolsky, W. Vetterling, Numerical Recipes, p. 687–693, (Cambridge University Press), (1986)
6. L. Lyons, Statistics for Nuclear and Particle Physicists, p. 62–63, (Cambridge University Press), (1986)

AN EVALUATION OF BATSE BURST LOCATIONS COMPUTED WITH THE MAXBC DATATYPE

T. M. Koshut, W. S. Paciesas, G. N. Pendleton
Dept. of Physics, University of Alabama in Huntsville, Huntsville, AL 35899

M. N. Brock, G. J. Fishman, C. A. Meegan, R. B. Wilson
Marshall Space Flight Center, ES 64, Huntsville, AL 35812

ABSTRACT

One of the primary objectives of BATSE is to determine the direction to each observed gamma-ray burst, allowing the angular distribution of the burst sources to be studied. Most of the BATSE burst data types are not suitable for this purpose, since they are produced by combining rates from several detectors (details of the BATSE experiment and the various datatypes can be found elsewhere[1,2]). After the loss of the CGRO tape recorders in March, 1992, the availability of data with rates from individual detectors has often been limited by telemetry gaps. Consequently, many burst directions are derived using the MAXBC data, which are almost always available, but have significant limitations. MAXBC data contain the maximum background-subracted count rate (counts per 64 ms) in the energy range of $\sim$ 50–300 keV, averaged over one second, for each of the eight Large Area Detectors. It is important to evaluate the locations computed using MAXBC data because these locations will appear in the BATSE 2B Catalog when no other data are available. We report on the comparison of burst locations computed using MAXBC data with locations derived from the Third Interplanetary Network[3], hereafter known as IPN[3]. We report on the comparison of MAXBC locations of hard solar flares with the known position of the Sun. We also report on the comparison of burst locations computed using MAXBC data with those locations given in the first BATSE catalog, for which the burst data are essentially complete.[4]

METHODOLOGY

The 11 gamma-ray bursts used in these comparisons were selected because each has been well-localized by the IPN[3]. The 22 solar flares were chosen because their spectra are harder than an average flare, thus closer to a typical burst spectrum. Moreover, the flares extend the intensity range of our sample of well-localized events further down than possible with only the IPN[3] bursts. These 33 events are the same events used in the analysis shown in Figure 2 of the BATSE 1B Catalog.

Three locations were calculated for each event. Details concerning the method of calculating locations, and the systematic and statistical errors involved, will not be discussed here but can be found elsewhere.[5,6] One of the three locations was determined using a power-law spectral index of 2.0. This value is used by the BATSE team when calculating locations of events for which there is no other suitable LAD data. Additionally, a value of 2.0 is used by the BATSE team when determining the preliminary location for a strong burst, with the intention of quickly alerting investigators observing at other wavelengths. The second location computed for each event employs a spectral index

obtained from a hardness ratio HR look-up table, with

$$HR = \frac{10000 \times Ch2}{Ch2 + Ch3} \tag{1}$$

where $Ch2$ and $Ch3$ are the background-subtracted count rates in the LAD discriminator channel 2 (spanning $\sim$ 50–100 keV) and discriminator channel 3 (spanning $\sim$ 100–300 keV) respectively. This method is used by the BATSE team when the preferred 16-channel CONTINUOUS data and 4-channel DISCLA data are not available due to telemetry gaps. The third location computed for each event utilizes the best-fit spectral index used in calculating the locations in the BATSE 1B Catalog.

The offsets (in degrees) of each location from the well-known locations were calculated. The offsets of each location from the published 1B Catalog location (for which the burst data are essentially complete) are also calculated. The values used for the 1B Catalog solar flare locations are the same values used to make Figure 2 of the 1B Catalog. In addition to locations, the signal-to-noise ratio in the 2 brightest detectors was calculated for each event. If one trys to compare Figure 2 of the 2B Catalog with the results presented here, it must be noted that the value of the signal-to-noise ratio for each event will not necessarily be the same. In the 1B Catalog we were able to use various data types, most of which provided better energy resolution than MAXBC, as well as more flexibility in choosing the burst time interval (recall that MAXBC are the background- subtracted rates only at the peak time of the burst in the 50–300 keV energy range).

RESULTS

Table I. provides a brief summary of the various location comparisons. The two samples being computed are given in the first two columns. The third column specifies the method used to obtain the power-law sepctral indices. The fourth column gives the mean total (systematic + statistical) error $\langle\sigma\rangle$, where

$$\langle\sigma\rangle = \frac{1}{N}\sum_{i=1}^{N}\sigma_i \tag{2}$$

and σ_i is calculated as the difference (in degrees) between the locations from each of the two samples, for the i^{th} event. N is the total number of events in the sample. The fifth column informs the reader which figure contains the corresponding comparison data.

Figure 1 shows the offset of the MAXBC locations from the well-localized locations plotted as a function of the signal-to-noise ratio in the two brightest detectors. The distinguishing characteristic for each of the three plots is the method used to obtain the power-law spectral indices. The dashed line in each figure is a representation of the statistical errors as calculated in the BATSE 1B Catalog.

Figure 2 shows the offset of the MAXBC locations from the locations given in the 1B Catalog plotted as a function of the signal-to-noise ratio in the brightest detectors. Again, the distinguishing factor between these three plots is the method used to obtain the power-law sepctral indices. The dashed line again represents the BATSE 1B Catalog statistical errors.

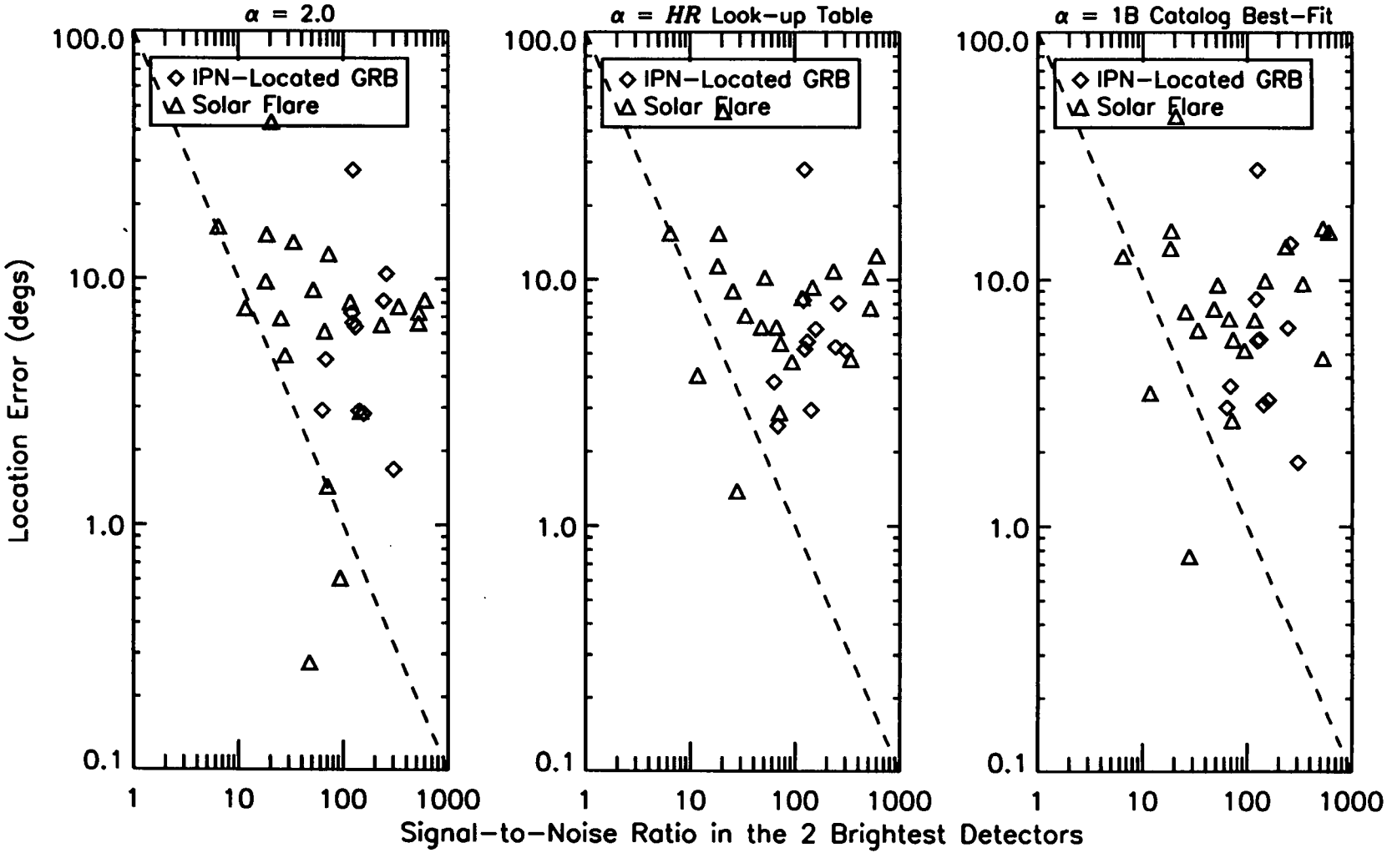
α = 2.0
α = HR Look-up Table
α = 1B Catalog Best-Fit
◇ IPN-Located GRB
△ Solar Flare
100.0
10.0
1.0
0.1
1
10
100
1000
Location Error (degs)
Signal-to-Noise Ratio in the 2 Brightest Detectors

Figure 1.

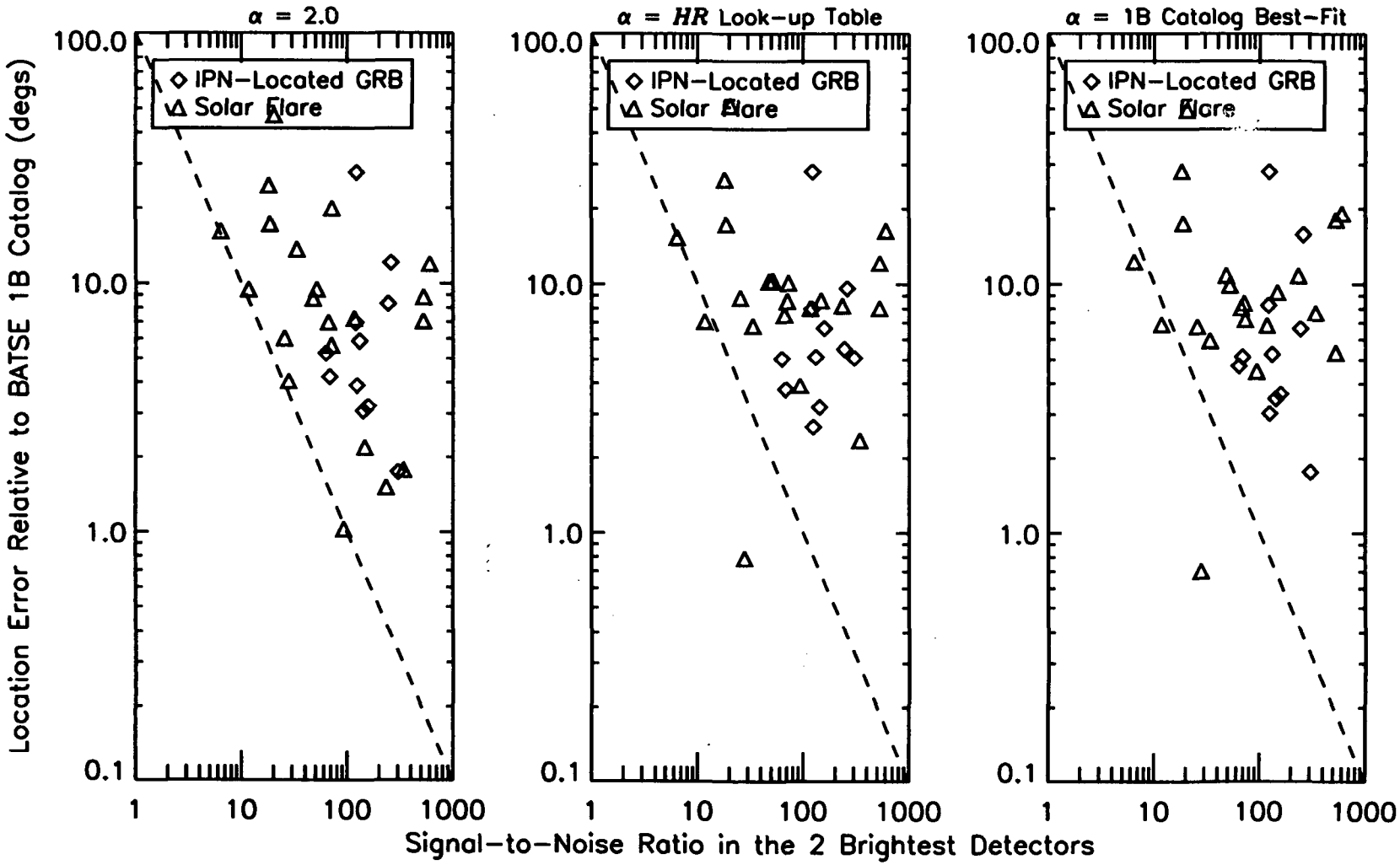
α = 2.0
α = HR Look-up Table
α = 1B Catalog Best-Fit
◇ IPN-Located GRB
△ Solar Flare
100.0
10.0
1.0
0.1
1
10
100
1000
Location Error Relative to BATSE 1B Catalog (degs)
Signal-to-Noise Ratio in the 2 Brightest Detectors

Figure 2.

FUTURE WORK

These results, combined with a more detailed analysis of the seperate systematic and statistical errors, will be included in the BATSE 2B Catalog.

Table I. Analysis of MAXBC Locations

MAXBC Sample	Comparison Sample	Power-Law Spectral Index	$\langle\sigma\rangle$ (degs)	Figure Number
Bursts	IPN Bursts	2.0	7.41	1
		HR Look-Up Table	7.39	
		1B Catalog Best-Fit	7.57	
Solar Flares	Sun Location	2.0	9.10	1
		HR Look-Up Table	9.80	
		1B Catalog Best-Fit	10.31	
Bursts	1B Catalog Locations	2.0	7.48	2
		HR Look-Up Table	7.52	
		1B Catalog Best-Fit	7.79	
Solar Flares	Figure 2 in 1B Catalog	2.0	10.73	2
		HR Look-Up Table	11.46	
		1B Catalog Best-Fit	11.83	

REFERENCES

1. G. Fishman et al., Proceedings of the Gamma Ray Observatory Science Workshop , 2-39 (1989).
2. J. Horack, NASA Reference Publication No. 1268 , (1991).
3. K. Hurley, private communication , (1993).
4. G. Fishman et al., Ap. JS , in press (1993).
5. M. Brock et al., Proc. Huntsville Gamma-Ray Burst Workshop (AIP, N. Y., 1991), p. 383.
6. M. Brock et al., Proc. Compton Gamma-Ray Observatory (AIP, N. Y., 1992), p. 709.

THE ENERGY EMISSION OF GAMMA-RAY BURSTS AND SOLAR FLARES

R.S. Mallozzi, G.N. Pendleton, T.M. Koshut, W.S. Paciesas, M.S. Briggs

Dept. of Physics, University of Alabama, Huntsville, AL 35899

ABSTRACT

A study of the continuum spectra of gamma-ray bursts (GRBs) and solar flares (SFs) is performed to investigate the photon energy flux of these events. BATSE 16 channel Large Area Detector (LAD) data are fit using a forward-folding model-fitting technique to produce photon spectra. The integral of the fit of each spectrum is used to compute the energy flux over consecutive intervals of the event, resulting in a time history of the power output (ergs/sec). These are compared to search for similarities among the emission mechanisms in GRBs and SFs. Comparison with the solar flare energy emission may yield information about the gamma-ray burst production site.

DATA AND ANALYSIS

The Burst and Transient Source Experiment (BATSE) consists of eight independent detector modules mounted on the corners of the Compton Gamma-Ray Observatory (CGRO), and is capable of nearly full-sky observations. This detector system, explained in detail elsewhere[1,2], provides continuous monitoring of the x-ray and gamma-ray sky. Each of the detector modules consists of two NaI(Tℓ) scintillation detectors: a Large Area Detector (LAD), optimized for temporal resolution, and a Spectroscopy Detector (SD), optimized for energy resolution.

We use the BATSE Continuous (CONT) and Medium Energy Resolution (MER) datatypes from the LADs. The CONT datatype, received in every telemetry packet, provides 2.048 second resolution in 16 energy channels spanning the range ~20–1800 keV; the MER datatype, accumulated only in burst mode and beginning ~30 ms after a trigger occurs, consists of 16 energy channels providing 16 ms resolution for ~32.8 seconds followed by 64 ms resolution for ~130 additional seconds. Thus MER data does not provide any pre-trigger information. Events which had significant emission before the trigger were, in general, analyzed with CONT data; events with fine time structure were analyzed with MER data to enable resolution of shorter spikes within longer events.

The data were deconvolved using a standard forward-folding model-fitting technique to produce photon spectra. Each event was divided into time intervals of equal duration and a photon spectrum was produced for each interval. The spectra were integrated over the fitted energy range (~20–1800 keV for GRBs and ~30–225 keV for SFs) to obtain the total photon and energy output during each interval, resulting in a time history of the photon and energy flux for that event. The flux histories of gamma-ray bursts and solar flares were compared to search for similarities among the two types of events. We find that the solar flare photon and energy flux histories are of almost identical shape, indicating little or no spectral evolution for these events. The gamma-ray bursts sometimes show significant differences between the photon flux and and the energy flux. This gives some information regarding the emission mechanism of the burst sources,

suggesting that the burst emission environment is not the same as that of solar flares.

The gamma-ray burst data were fit with a normal distribution in $\log_{10}$ energy (E) with variable (linear function of energy) width over the ~20–1800 keV range:

$$\frac{dN}{dE} = \frac{\mathrm{A}}{\sigma_g\sqrt{2\pi}} \exp\left\{-\frac{1}{2}\left[\frac{\log_{10}(E) - \log_{10}(E_{\mathrm{cent}})}{\sigma_g}\right]^2\right\} \qquad (1)$$

where

$$\sigma_g = \frac{\log_{10}\big(FWHM(E)\big)}{2.35482},$$

and

$$\log_{10}\big(FWHM(E)\big) = \sigma(E_{\mathrm{cent}}) + \Delta\sigma(E_{\mathrm{cent}}) \times \big(\log_{10}(\mathrm{E}) - \log_{10}(\mathrm{E_{cent}})\big).$$

There are four varying parameters in this model: A denotes the amplitude, E_{cent} the energy of the centroid, $\sigma(E_{\mathrm{cent}})$ the full width at half maximum ($FWHM$) of the Gaussian, and $\Delta\sigma(E_{\mathrm{cent}})$ the change in the full width with energy. This function fits the wide range of observed gamma-ray burst spectra well, keeping in mind that we are not strictly concerned with the model that is used, but only that the function represents the data reasonably well. Therefore this functional form is adequate to ensure that the integral is descriptive of the actual energy output. The solar flare data were fit with a simple power law over the ~30–225 keV range:

$$\frac{dN}{dE} = A\left(\frac{E}{E_0}\right)^{-\alpha} \qquad (2)$$

with E_0 fixed at 100 keV. A is the amplitude of the function, and α is the power-law index (generally ~3–6 for the solar data examined here). Limiting the energy range over which the solar flare data were fit enabled a straight power law to sufficiently describe the spectra of these events. The power law fits to the solar data sometimes exhibited large χ^2 during the most intense portions of the events due to the excellent counting statistics at these times.

RESULTS

The analysis was performed for 15 solar flares and 11 gamma-ray bursts observed by BATSE. Although the sample sizes were limited, we attempted to select events which differed significantly in their time histories. Eight of the 15 solar flares were visible above ~100 keV, the remainder showing emission only below ~100 keV. Seven of the 11 gamma-ray bursts showed significant emission above ~300 keV.

For emission produced by a single mechanism, the absence of extreme spectral evolution implies that the energy flux history closely mimics the photon flux history. The solar flares examined exhibited this property, supporting observations made with the Gamma-Ray Spectrometer (GRS)[3] on the Solar Maximum Mission (SMM), which showed that the hard x-ray (~10–140 keV) and γ-ray (~10–100 MeV) fluxes peak within ~one second of each other. It has

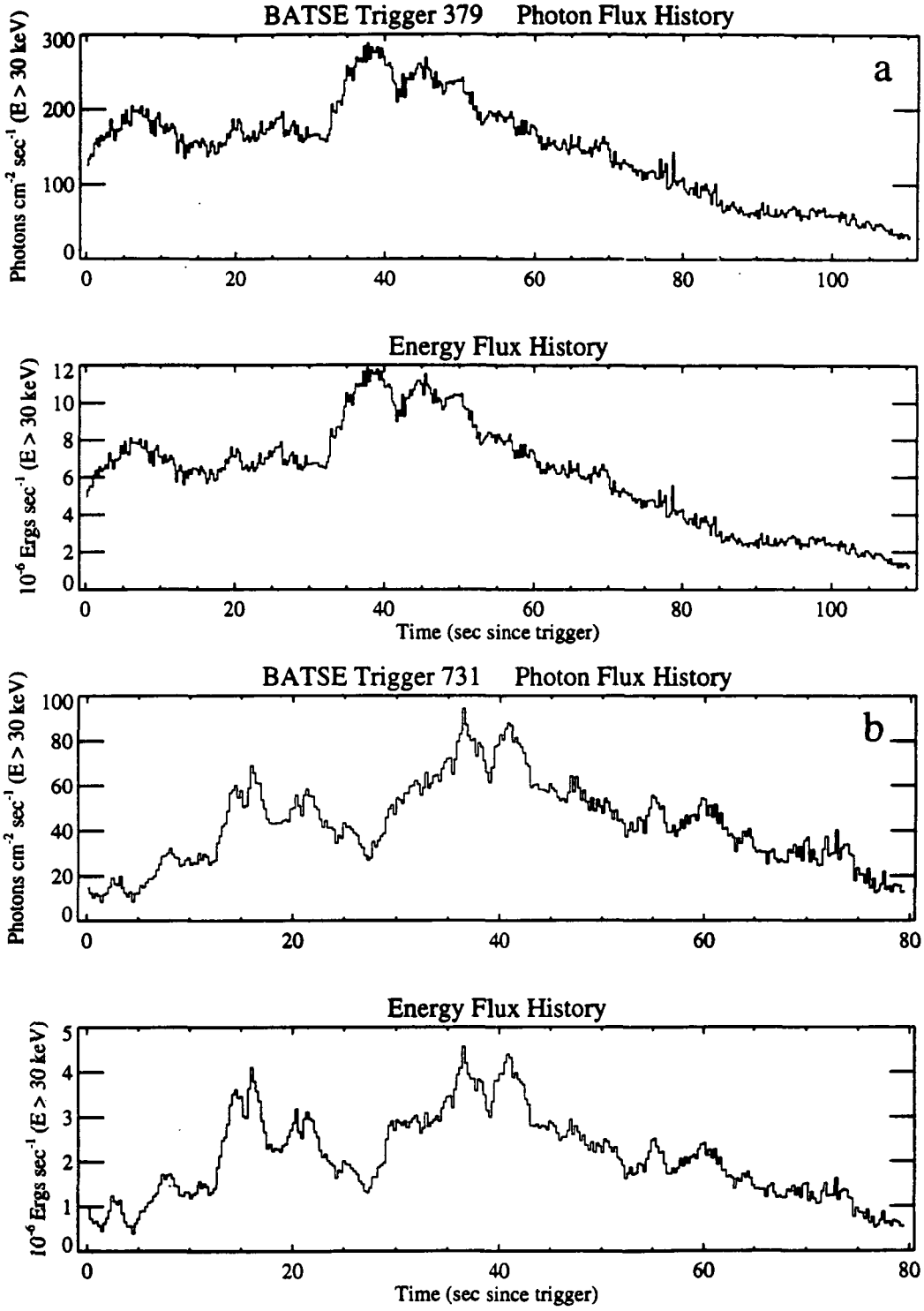

Figure 1. Solar Flares

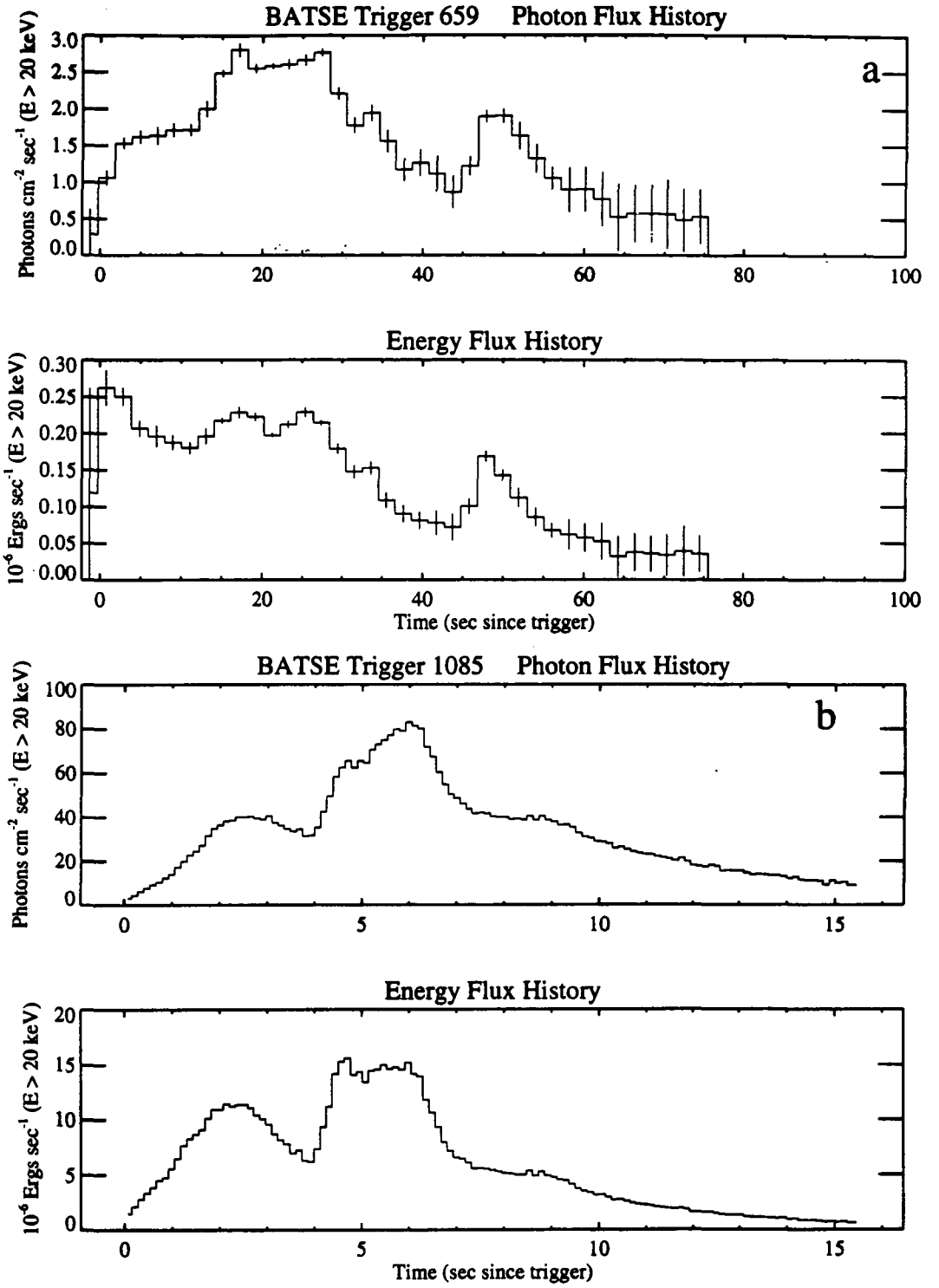

Figure 2. Gamma-Ray Bursts

also been shown that the radio flux peaks near this time as well (see reference 4 and references therein). Figure 1 shows two typical examples of the flares which were analyzed, demonstrating the excellent correlation between photon flux and energy flux. It should be noted that it is possible for the two varying parameters of the power law model used to fit the solar data to change in such a manner that the energy evolution follows the photon evolution.

Several of the gamma-ray burst profiles appear to exhibit a more pronounced rise in the energy flux followed by a steady decay even though the photon flux may be increasing (see Figure 2a). The burst shown in Figure 2a reaches its maximum in energy at the start of the event, while the photon flux peaks at approximately 20 seconds later. The smooth gamma-ray burst shown in Figure 2b reveals particularly intriguing features in its energy output evolution. The energy reaches maximum quickly, then remains relatively constant for several seconds, implying sustained energy injection or lack of energy dissipation in the burst environment. There is also a striking exponential decay in energy at the end of the event, although the count rate history also shows feature.

CONCLUSIONS

Although the photon and energy fluxes are strongly correlated, examination of the energy output of solar flares and gamma-ray bursts suggests that the emission environments of the two types of events are, in general, not identical. Several of the gamma-ray bursts reveal intriguing differences between the photon output and the energy output. Observations with the BATSE Spectroscopy Detectors in conjunction with those of the LADs support the hypothesis of two separate photon production mechanisms in solar flares: thermal ($\lesssim$10 keV) and thick-target ($\gtrsim$10 keV) Bremsstrahlung. The diversity in the temporal profiles of GRBs with energy suggests that these events are also the result of two or more photon production mechanisms, albeit mechanisms which appear to be distinct from those responsible for solar flares. Comparison of the solar and gamma-ray burst photon and energy flux histories support this suggestion.

REFERENCES

1. Fishman, G.J. et al., Proceedings of the GRO Science Workshop, ed. W.N. Johnson (NASA/GSFC, 1989), p. 2-39.
2. Horack, J.M., Development of the Burst and Transient Source Experiment, NASA-RP 1268 (1991).
3. Forrest, D.J. et al., Solar Phys., **65**, 15-23 (1980).
4. Aschwanden, M.J., et al., ApJ, **417**, 790-804 (1993).

Continuum Spectral Characteristics of Bursts Measured with the BATSE Large Area Detectors

G. N. Pendleton, W. S. Paciesas, M. S. Briggs
R. S. Mallozzi, T. M. Koshut
University of Alabama in Huntsville
G. J. Fishman, R. B. Wilson, C. A. Meegan
NASA/Marshall Space Flight Center
C. Kouveliotou
Universites Space Research Association

ABSTRACT

The continuum spectra of bursts are studied with particular emphasis placed on the search for spectral subcomponents. The spectra observed in individual bursts show significant evolution throughout their durations. This study addresses the degree to which hard and soft spectra are combined in bursts and the effect this has on the complexity of the observed spectra. In particular it is shown that the presence of broad cusps in spectra in the 40-100 keV range can be explained by the superposition of hard and soft spectra in the bursts. This interpretation is not meant to explain narrow spectral absorption lines in bursts. It is simply an alternate explanation for some of the broader features observed in the continuum spectra of GRBs.

INTRODUCTION

Gamma-ray bursts are known to exhibit a wide range on continuum spectra[1]. Spectral variation is not only seen between bursts but within bursts as well[2,3]. Bursts have been observed with narrow absorption and emission lines in them as well as with broader features of this type[1,2,4,5,6]. This work shows that broad absorption features in the 40-100 keV range can be explained by the superposition of hard and soft burst continuum spectra. These results are important for estimating the frequency with which absorption line features should be observed in gamma-ray burst continuum spectra. It also has implications for the temporal behavior of the energy release mechanisms operating in bursts.

PROCEDURE AND DATA ANALYSIS

The medium energy resolution (MER) data from the BATSE[7] instrument, consisting of 16 channel Large Area Detector (LAD) data in the 20-2000 keV energy range with up to 16 ms time resolution, were used for the bulk of this analysis. The LAD spectra were compared for consistency to the spectroscopy (SD) detector data and were found to be in agreement.

The main spectral continuum model used here is a generalized form of the lognormal distribution. It is a gaussian of the log of the energy where the full width half maximum (FWHM) is a linear function of the log of the energy. This

is a very flexible functional form that will fit spectra that do not have a change in the sign of their curvature in the interval being fit. Its mathematical form is presented in detail elsewhere[8].

The channel to energy conversion for the LAD 16 channel data has been optimized[9] using in-flight calibration data to remove systematic effects from the spectral analysis.

Figure 1 shows two very different spectra observed in the same burst fit with the model described above. Figure 1A shows the continuum spectrum for the first 1.2 s of BATSE trigger 907 (1B 911007) while figure 1B shows a 1.2 s spectrum 117.5 s into the burst. The superposition of these two spectra would produce a cusp or broad absorption feature in the resulting spectrum.

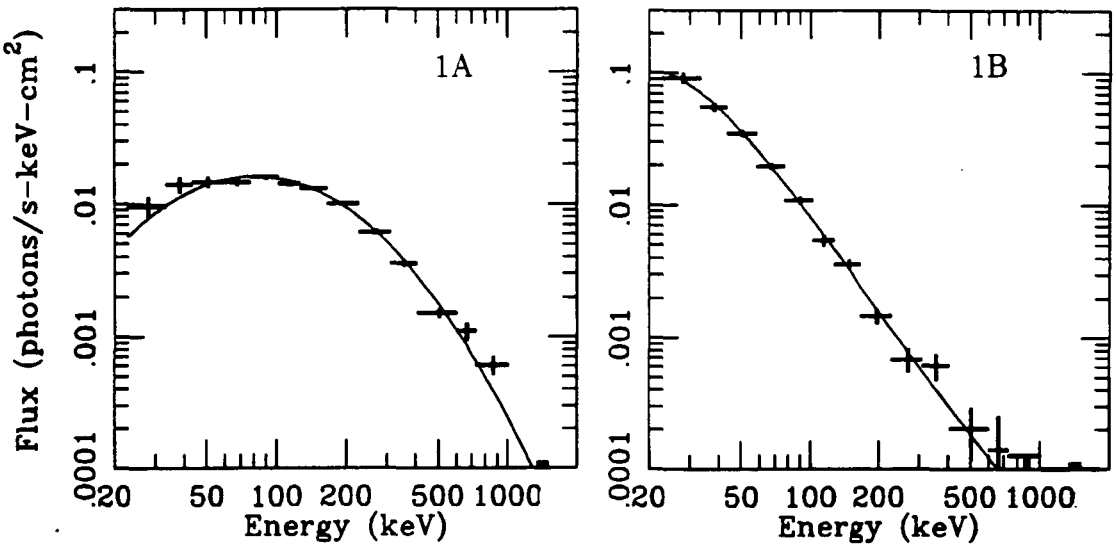

Figure 1: Spectral fits for two separate intervals of trigger 907 (1B 911007)

The obvious next step is to inspect the time profiles of the bursts to find intervals where the onset of hard Figure 1A type emission is preceded by softer emission and see whether significant cusps are visible in the spectra. Figure 2 shows the time profiles of the counts spectra of trigger 1025 (1B 911109) in four broad energy channels. These are the LAD discriminator data. In this burst there is an episode of hard emission 2s after the burst trigger lasting 0.3 s, as is evident in the E > 300 keV time profile. The 20-50 keV time profile shows a fairly gradual rise in counts from the trigger time until the hard outburst. Furthermore no feature corresponding to the hard episode is visible in the 20-50 keV range.

In order to test for the significance of two spectral component superposition in any of the spectra comprising this burst the MER data were summed into 0.2s intervals over the duration of the event. These spectra were then fit with the generalized lognormal described above for each interval. Then the Sunyaev-Titarchuk Comptonization model was added to the generalized lognormal and

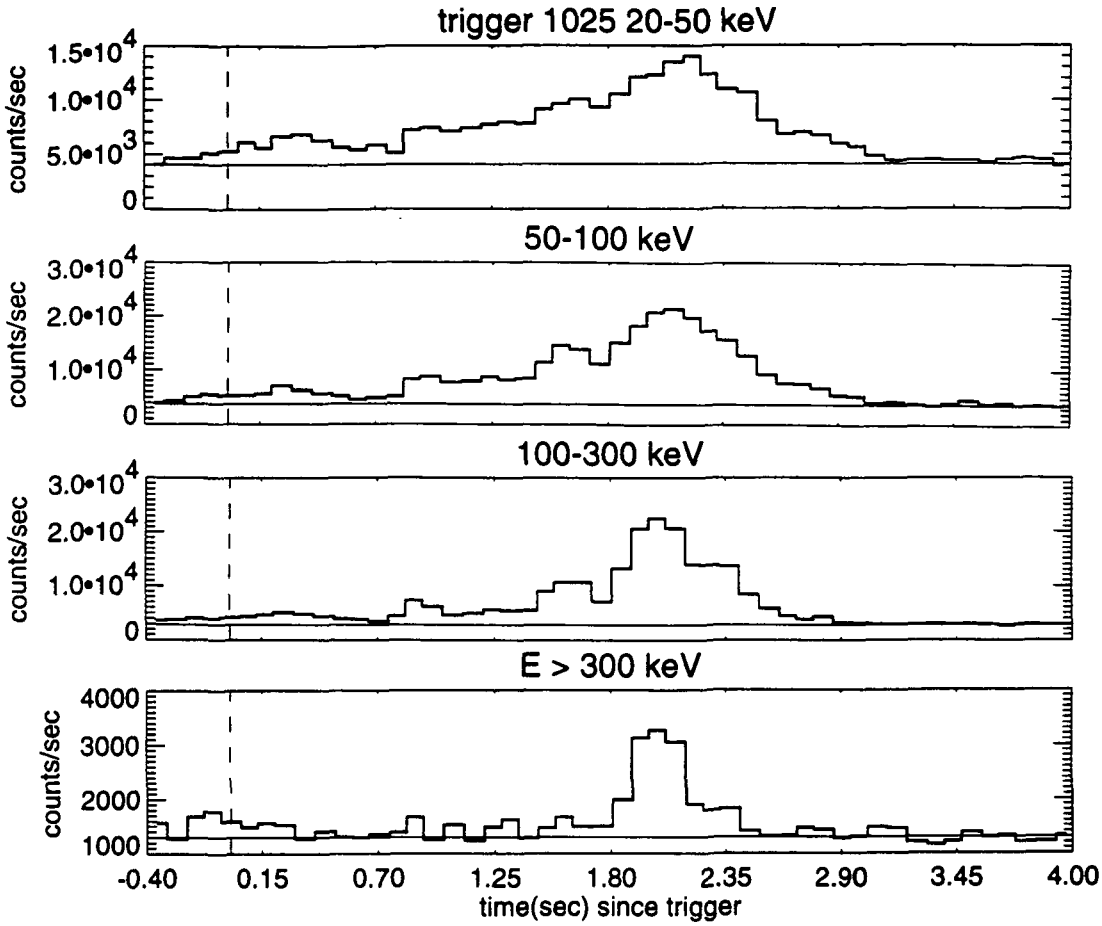

Figure 2: Time profiles of trigger 1025 (1B 911109)

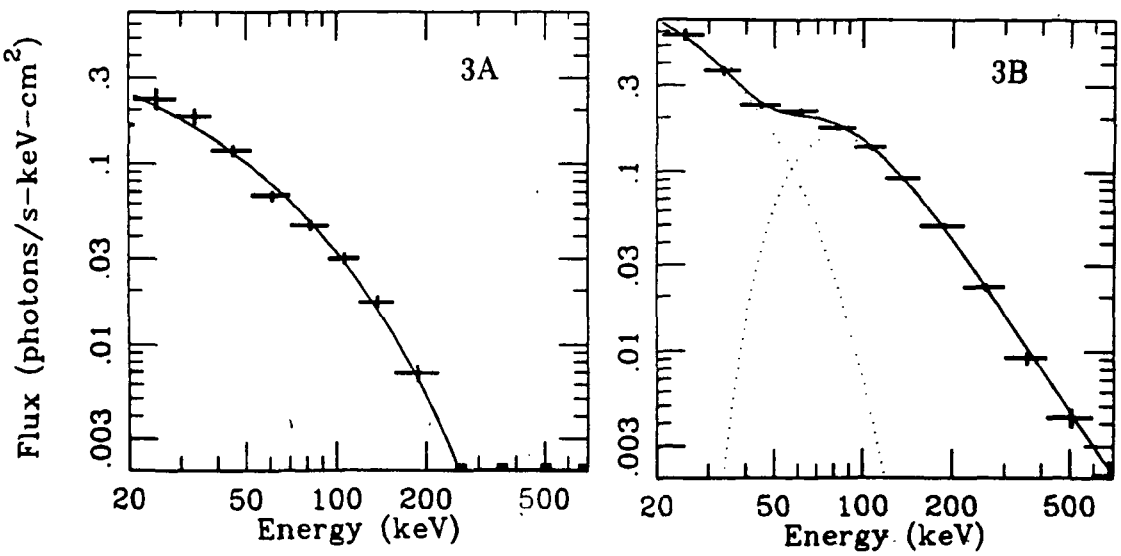

Figures 3A and 3B: Spectral fits for two separate intervals of trigger 1025 (1B 911109)

the fitting was repeated. The F-test was then performed on each interval to see if the addition of the Sunyaev-Titarchuk Comptonization model produced a significant improvement in the fit. The improvement was significant at the 1% level (i.e. a 1% chance that the improvement was incidental) for the 2.0-2.2s interval and at the 5% level for the two intervals preceding it. All the other intervals showed no significant improvement even though many of these intervals had source count rates comparable to the intervals showing two component structure. The 16 channel, 2.048 s resolution LAD data for each separate detector showed the significance of the added continuum component as well. The SD detector data were consistent with the LAD data although not as statistically significant.

Figure 3A shows a spectrum from the 1.2-1.4 s interval of trigger 1025 fit with the generalized lognormal acceptable at the 10% level (i.e. the model will produce a data set like this at least 10% of the time). Addition of the Sunyaev-Titarchuk model yields no significant improvement. Figure 3B shows the 1.9-2.1 s interval of trigger 1025 fit with the generalized lognormal and the Sunyaev-Titarchuk model acceptable at the 10% level. The generalized lognormal fit alone is only acceptable at the 5.0×10^{-5}% level. The F-test shows that the addition of the Sunyaev-Titarchuk model is a significant improvement for this interval at the 1% level.

Another burst that shows some broad cusp-like structure in the first second after reaching trigger threshold is 1085 (1B 911118). Figure 4A shows the photon spectrum for the first 0.0-0.25 s interval of the burst fit to the generalized lognormal. Figure 4B shows the counts spectrum for the same fit to demonstrate the presence of the structure in counts space. Although the generalized lognormal fit in the 20 to 300 keV range cannot be ruled out since it is acceptable at the 8% level, the F-test shows that the addition of the Sunyaev-Titarchuk model is a significant improvement for this interval at considerably greater than 1% level. The pattern of evolution of this burst over the first second since trigger is one where a hard component grows in intensity until it buries the softer emission obscuring the cusp-like feature present in the first quarter second.

DISCUSSION

This is not the first time that multiple spectral components have been proposed for bursts[10] or the first time that the superposition of spectral components has been proposed as an explanation for some of the broad, absorption line-like features observed in bursts[11]. The BATSE LAD data provide us with an opportunity to study the evolution of spectral components and absorption lines with good statistics and see which explanation fits the observations most convincingly. It seems unlikely that the superposition of spectral components could explain narrow absorption features that have been observed with other instruments[5], however it could explain some of the more complicated looking spectra found in the Konus Catalog[1]. Determining how many of the previous observations of lines are clearly narrow absorption lines vs. broad cusps is important for determining how likely it

tinuum spectra. Studying the comparative evolution of hard and soft components in bursts may yield valuable insights into the physical mechanisms that produce the observed spectra. For instance the time profile of trigger 1025 clearly shows the onset of hard emission after the burst process has been initiated. This shows that the bursts do not evolve uniformly from hard to soft and indicates that hard emission process can trigger repeatedly during a burst's output. Studying the development of the bursts' spectra should help map out the characteristics of this as yet unexplained physical phenomenon.

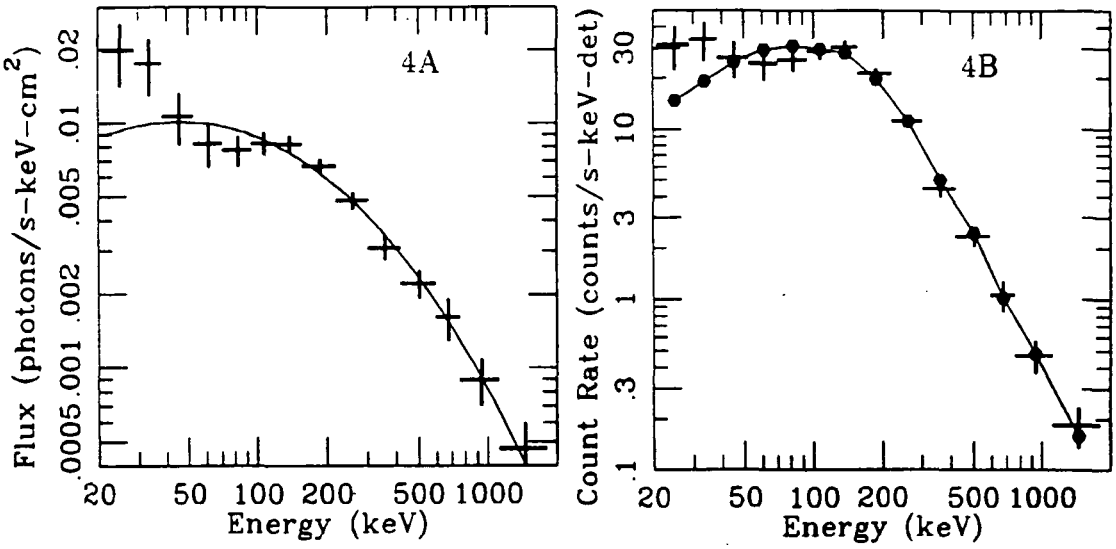

Figures 4A and 4B: Spectral fits for the same interval of trigger 1085 (1B 911118) in units of photons and counts.

REFERENCES

1. Mazets et al, 1981, Astophys.Space Sci. 80:3-143
2. Mazets et al, 1982, Astophys.Space Sci. 82:261-282
3. Mitrofanov et al, 1984, Sov. Astron. AJ 28:547-49
4. Teegarden et al, 1980, Ap J. Lett. 236:L67-70
5. Murakami et al., 1988, Nature 335:234-35
6. Golenetskii et al 1986,Astrophys. Space Sci. 124:243-78
7. Fishman et al, 1989 in proceedings of the GRO Science Workshop, ed. N. Johnson, pp. (2)39-2(50)
8. Mallozzi et al, these proceedings.
9. Pendleton et al, proceedings of the second compton symposium. Sept 20-22, 1993, U. Maryland, in press.
10. Mitrofanov et al, 1992 in Gamma-Ray Bursts: Observations, Analyses, and Theories, Ed. C. Ho, R. Epstein, and E. Fenimore, pp. 209-216
11. Fenimore et al, 1982 in Gamma Ray Transients and Related Astrophysical Phenomena, Ed. R. Lingenfelter, H. Hudson, and D. Worrall

CN22 (0) (2)
TURNER J/PUBLICATION
MARSHALL SPACE FLIGHT CENTER
HUNTSVILLE AL.

DELETIONS OR CHANGES 544-4494
RETURN ADDRESS CN22D 000002444